

1           **Interpreting scattered *in-situ* produced cosmogenic nuclide depth-profile data**

2

3

4   **K. Le Dortz**<sup>1,2,3\*</sup>, **B. Meyer**<sup>1,2</sup>, **M. Sébrier**<sup>1,2</sup>, **R. Braucher**<sup>4</sup>, **D. Bourlès**<sup>4</sup>, **L. Benedetti**<sup>4</sup>,  
5   **H. Nazari**<sup>5</sup>, **M. Foroutan**<sup>1,2,5</sup>

6

7

8   1- UPMC Univ Paris 06, ISTEP, UMR 7193, F-75005, Paris, France

9   2- CNRS, ISTEP, UMR 7193; F-75005, Paris, France

10   3 - Laboratoire de Géologie, ENS, UMR 8538, 75231 Paris

11   4 - *CEREGE, UMR 6635 CNRS-Aix Marseille Université, 13545 Aix-en-Provence, France*

12   5- Geological Survey of Iran, Teheran, Iran

13

14   \*Corresponding author : Phone : 0033144322275, Fax : 0033144322200 Email :

15   ledortz@geologie.ens.fr

16

17

18   ***Abstract***

19   Modelling the evolution of the concentration of *in-situ* produced cosmogenic nuclides as a  
20   function of depth (depth-profile) has been developed to allow determining both the exposure  
21   duration and the denudation rate affecting geomorphic features. However, material sampled  
22   through surficial deposits may exhibit an inherited component resulting from exposure to  
23   cosmic rays before deposition. In case of homogeneous inheritance, this inherited component  
24   may be estimated through sampling at increasing depths and subsequently subtracted. In case  
25   of variable inheritance, the measured concentrations are scattered and the random distribution  
26   of the depth-profile concentrations prevents modelling confidently a depth-profile and  
27   precludes constraining an exposure duration. Often observed in desert and endorheic regions,  
28   this greatly restricts the possibilities to determine an accurate abandonment age of alluvial  
29   surfaces in such environments. Provided the denudation is demonstrated negligible, a method  
30   for determining a more accurate range of minimum inheritance, hence a more accurate  
31   maximum abandonment age for a given alluvial surface, is proposed. This method, based on  
32   the rejuvenation of depth-profile samples, relies on the simple hypothesis that at least one of  
33   the depth-profile samples would be emplaced with no or negligible inherited component and  
34   on the obvious principle that none of analyzed sample has been emplaced with a negative

35 cosmogenic nuclide concentration. The method consists then in determining which of the  
36 measured depth-profile sample may have been emplaced with a null CRE concentration; i.e.,  
37 with a zero inheritance value. This requires to calculate the *in-situ* duration of exposure  
38 needed to reach the concentration measured for each depth-profile sample and to retain the  
39 one that provides the smallest *in-situ* exposure duration. Several examples from alluvial  
40 surfaces of central Iran illustrate the profile rejuvenation method and highlight a variable  
41 inheritance ranging between  $1.5 \times 10^5$  and  $16.1 \times 10^5$  at/g ( $\text{SiO}_2$ ) for terraces whose  
42 abandonment ages range from ten to several hundreds of ka.

43

44

#### 45 **Introduction**

46 Cosmic ray exposure (CRE) dating has been widely used to estimate the age of  
47 alluvial surfaces in many regions worldwide. For a long while and still for some recent  
48 studies, surface samples only were collected to determine CRE ages (e.g., Ritz et al., 1995,  
49 Regard et al., 2006, Van der Woerd et al., 2006). Measurement of their cosmogenic nuclide  
50 concentration (most often  $^{10}\text{Be}$ ) yields a CRE age for each collected pebble (Figure 1a, upper  
51 panel). If enough pebbles have been collected on a given surface, a suitable statistical  
52 treatment may exhibit a Gaussian distribution centred on the weighted mean age eventually  
53 assigned to the studied surface (Figure 1b, upper panel). Sometimes, the measured  
54 concentrations are scattered and their distribution is multimodal (Figure 1c, upper panel). The  
55 occurrence of outliers resulting either from pre- or post-depositional processes is thus  
56 extensively discussed. While some authors point to denudation and artificial rejuvenation of  
57 the surface and favour the oldest ages (e.g., Brown et al., 2005), others point to inheritance  
58 and artificial ageing of the surface and therefore favour the youngest ages (e.g., Mériaux et  
59 al., 2005; Vassallo et al., 2007). Pre-depositional exposure indeed implies the accumulation of  
60 an inherited component that shifts the final Gaussian distribution towards greater  
61 concentrations while post-depositional denudation brings to the surface less concentrated sub-  
62 surface pebbles that widens and shifts the Gaussian distribution towards smaller  
63 concentrations. Neither the inherited component, nor the denudation rate can be estimated  
64 using surface samples only. In an attempt to clear up this point, depth-profile sampling has  
65 often been undertaken (Figure 1a, lower panel). Providing that the material constituting the  
66 deposit of interest has been emplaced over a short period of time, some ka, with respect to the  
67 subsequent duration of exposure and that it has been homogeneously pre-exposed, the depth-  
68 profile samples, whether individual or amalgamated pebbles, exhibit an exponential decrease

69 of their concentration as a function depth controlled by the attenuation length of the producing  
70 particles (e.g., Anderson et al., 1996; Repka et al., 1997). An exponential tending  
71 asymptotically to zero indicates no inherited component, while an exponential tending  
72 asymptotically to a characteristic concentration indicates a homogeneously distributed  
73 inherited component whose concentration is given by the asymptotically reached value  
74 (Figure 1b, lower panel). A chi-square inversion minimising the difference between the  
75 measured and modelled concentrations is often used to constrain from these depth-profiles the  
76 exposure duration of the studied surfaces, their denudation rate, and the concentration of their  
77 inherited components, if homogeneous (e.g., Siame et al., 2004; Braucher et al., 2009). Where  
78 the number of surface samples is limited or the distribution of their concentrations  
79 multimodal, depth-profiles also help narrowing the range of possible surface ages (e.g.,  
80 Nissen et al., 2009; Champagnac et al., 2010). However, scattered surface pebble  
81 concentrations are sometimes observed together with random depth distributions of  $^{10}\text{Be}$   
82 concentrations (e.g., Le Dortz et al., 2009). In such cases (Figure 1c), the distribution of  
83 surface pebbles is multimodal and the concentrations of the depth-profile samples do not  
84 decrease exponentially with depth, suggesting a variable inheritance and making any  
85 conventional modelling useless.

86 We have investigated such situations encountered in the desert region of central Iran  
87 while analysing offset fan surfaces along the Dehshir (Le Dortz et al., 2011) and Anar (Le  
88 Dortz et al., 2009) faults. Although sands appear to be less sensitive to inheritance than  
89 gravels (e.g., Matmon et al., 2005; Schmidt et al., 2011), the overall low sand content in the  
90 investigated alluvial material precluded the possibility to perform depth profile analysis on  
91 sandy material. Consequently, it was appropriate to collect samples of comparable  
92 granulometries (pebbles and cobbles) on the surface and all along depth-profile. To account  
93 for the scattering of cosmogenic nuclide concentrations and to determine the possible ranges  
94 of both the abandonment ages of the analyzed fan surfaces and the inheritance carried by their  
95 gravels, a CRE procedure has been developed. This procedure is based on depth-profile  
96 analyses, whose results are subsequently compared to the overlying surface samples. Such a  
97 procedure reveals appropriate because the studied sites met two necessary conditions: (1) the  
98 negligible denudation rate of the fan surface implies that depth-profile concentrations only  
99 depend on two unknowns (pre-exposure and *in-situ* exposure), and (2) the common source of  
100 alluvial material for both the surface and depth-profile samples implies that depth-profile  
101 samples can be compared with surface ones. The scatter of the measured cosmogenic nuclide  
102 concentrations resulting thus only from a variable inheritance, the concentrations calculated

103 using the proposed depth-profile rejuvenation procedure allow estimating a maximum  
104 abandonment age for a given fan surface and provide a range of minimum inheritance. The  
105 complete description of the sites, the sampling strategy, the details of the performed analyses,  
106 and the modelled ages can be retrieved in two previous papers (Le Dortz et al., 2009; Le  
107 Dortz et al., 2011). Some of these pebble data are used here to illustrate and discuss the  
108 limitations of a method, the profile rejuvenation procedure, which accounts for the variability  
109 of inheritance where denudation is negligible.

110

111

### 112 ***1. Profile rejuvenation methodology.***

113 Scattering of cosmogenic nuclide surface concentrations at a given site may result  
114 from both denudation processes and/or variable inheritance. At the Dehshir and Anar sites,  
115 qualitative observations of a desert pavement covering the very pristine surface of the fans  
116 made of varnished clasts suggested low erosion rate. This is quantitatively confirmed  
117 measuring the concentrations of two distinctive cosmogenic nuclides having different half-  
118 lives,  $^{10}\text{Be}$  (1.387 Ma; Chmeleff et al., 2010, Korschinek et al., 2010) and  $^{36}\text{Cl}$  (0.301 Ma;  
119 e.g., Gosse & Philipps, 2001) in samples along depth-profiles from the same oldest surface.  
120 The  $^{36}\text{Cl}$  ages calculated assuming no denudation and no inheritance are systematically  
121 younger than the  $^{10}\text{Be}$  ages calculated under the same assumptions, indicating that the  
122 carbonates samples had nearly reached the steady-state equilibrium - cosmogenic nuclide  
123 production balanced by losses due to radioactive decay and denudation, if any - at which the  
124  $^{36}\text{Cl}$  concentration only depends on the denudation rate. Modelling then the evolution of the  
125  $^{36}\text{Cl}$  concentrations along the depth-profiles quantitatively confirmed a denudation rate lower  
126 than  $10^{-3} \text{ mm.yr}^{-1}$ , hence negligible, over the investigated time span (Le Dortz et al., 2011).

127 Even if denudation rate is negligible, the original distribution of the pebbles at the surface of a  
128 terrace may be modified since their abandonment on the tread due to their closeness to the  
129 risers between two terrace levels, local overfloodings (e.g., Van der Woerd et al., 1998) or  
130 surface runoff, and diffusion (Owen et al., 2011). Sampling far from the risers may help  
131 mitigating such effects. However, one cannot rule out that a few of the pebbles collected at  
132 the surface might have been brought by animals or shepherds either from higher or lower,  
133 hence older or younger, levels. Such modifications are excluded for material deeper in a  
134 terrace. Unless biopedoturbation, ploughing or cryoturbation has modified the original  
135 relative depth position of some pebbles within the terrace material (Frankle et al., 2011), the  
136 samples collected at depth do represent the original relative depth distribution of the terrace

137 material. Clearly, there is no evidence for significant biopedoturbation, ploughing, or  
138 cryoturbation in the desert environment prevailing in central Iran. If it were, amalgamating  
139 10-30 individual pebbles for each depth-profile sample would ensure diluting the  
140 contributions of a few anomalous pebbles. Considering all the above-mentioned remarks, the  
141 scatter of cosmogenic nuclide concentrations (Figure 2a) measured both at the surface and  
142 along depth-profiles at several sites in central Iran should only result from two unknown  
143 contributions: the *in-situ* cosmogenic nuclide production and the pre-exposure of the analyzed  
144 samples. To limit these contributions, we propose to determine the minimum range of  
145 inheritance of a terrace, and consequently its maximum abandonment age, analyzing first the  
146 depth-profile samples. Providing that the terrace aggraded during a short time interval coeval  
147 with a single climatic crisis, as confirmed by OSL ages within some of the alluvial terraces  
148 (Le Dortz et al., 2011) and was not subsequently affected by significant denudation, the  
149 measured depth-profile concentrations should only result from *in-situ* production and pre-  
150 exposure. Then the proposed method relies on the impossibility for any depth-profile samples  
151 to have been emplaced in the terrace material with a negative cosmogenic nuclide  
152 concentration. Thus, considering the sampling depth and assuming that the measured  
153 concentration would only results from *in-situ* production (i.e., the sample would have been  
154 emplaced with a null cosmogenic nuclide concentration), one can calculate the time needed to  
155 bring back to zero each depth-profile concentration. The maximum abandonment age  
156 corresponds to the time needed for the depth-profile sample, which could be brought back  
157 from its measured concentration to a null concentration without bringing the other depth-  
158 profile samples to a negative concentration (Figure 2b, step 1). Therefore, this method is  
159 based on the simple hypothesis that, if denudation is negligible, at least one of the depth-  
160 profile samples could be emplaced with no inherited component. Subtracting for each profile  
161 sample the concentration accumulated at its sampling depth during the thus estimated  
162 maximum abandonment age to the measured concentration yields excess concentrations that  
163 correspond, when corrected for radioactive decay since the maximum abandonment age, to  
164 the minimum inherited components

165 The accuracy of the maximum abandonment age deduced from the profile  
166 rejuvenation method may then be evaluated through its comparison with the abandonment  
167 ages deduced from the concentrations measured in the individual pebbles or cobbles collected  
168 on the terrace tread. However, a prerequisite to such comparison is to ensure that the material  
169 sampled at a given site along a depth-profile and on the fan surface originates from the same  
170 source. For two (Anar and Dehshir North) out of three of the analyzed sites, the geologically

171 homogeneous catchment areas are small enough to reasonably postulate a short transport  
172 duration of the alluvial material. In addition, approximately 4-m-high natural or excavated  
173 outcrops within the alluvial sediments do not evidence significant change of gravel source  
174 during the fan aggradation. Thus, it is qualitatively unlikely that the source of the alluvial  
175 material changed during the emplacement of the near-surface and surface samples. To  
176 validate these field observations, an *a posteriori* statistical comparison of the concentrations  
177 measured at the surface with those measured along depth-profiles was performed at each  
178 analyzed site (see Appendix and following sections). The maximum abandonment age  
179 determined using the profile rejuvenation method allows calculating a maximum surface  
180 concentration at each given sampling site according to its spatial coordinates. Adding that  
181 maximum concentration to that found in excess in each profile sample, when using the same  
182 rejuvenation procedure (see above), yields to surface equivalent calculated concentrations that  
183 thus represent the concentrations that would have been measured if the samples collected  
184 along the depth-profile had been exposed solely at the surface. Finally, these calculated values  
185 are compared to the concentrations measured in the surface samples. Because nearly all the  
186 calculated concentrations fall in the range of those measured at the surface this implies that  
187 samples from depth-profiles and surfaces originate at each site from the same source.  
188 Therefore, we consider that the amalgam depth-profile concentrations represent the average  
189 concentration that would yield multiple sampling of pebbles at a given depth and the scatter  
190 of concentrations between successive amalgams corresponds mainly to the variability of  
191 inheritance among a homogeneous source. This scatter of concentrations along depth-profiles  
192 corresponds then only to variable pre-exposure duration in the upper catchments, and the  
193 accuracy of the maximum abandonment age of the fan surface determined using the profile  
194 rejuvenation method may thus be compared to the surface concentrations (Figure 2c, step 2).  
195 Thus, if most concentrations of the surface pebbles become negative while subtracting the *in-*  
196 *situ* concentration that would have been accumulated at the surface during the duration that  
197 corresponds to the maximum cosmogenic nuclide abandonment age determined from the  
198 profile rejuvenation, then that maximum abandonment age is not physically acceptable  
199 (Figure 2c, right). On the contrary, if most of these surface concentrations remain positive by  
200 performing the same operation, the maximum cosmogenic nuclide abandonment age ( $t_{\text{Max}}$ )  
201 provides a maximum possible age for the fan surface (Figure 2c, left).

202 Finally, a minimum cosmogenic nuclide abandonment age ( $t_{\text{min}}$ ) can be estimated from  
203 the lowest surface concentration (Figure 2d, step 3) that, in addition, allows estimating the  
204 maximum range of inheritance values for such a  $t_{\text{min}}$ . This minimum cosmogenic nuclide

205 abandonment age may be compared with OSL ages, if available, to discuss whether it still  
206 could be affected by some inherited component. The following examples highlight the  
207 variability of the inheritance and illustrate the methodology to account for this variability and  
208 derive accurate limits on the inheritance and hence on the possible range of abandonment ages  
209 of a given alluvial terrace unaffected by denudation.

210

## 211 ***2. Estimating the ranges of inheritance and abandonment age on an alluvial terrace***

212 To illustrate the principles of the proposed methodology, samples from an  
213 intermediate terrace emplaced by the Marvast river at the Iranian Dehshir South site (T2  
214 terrace; Le Dortz et al., 2011) are used (Figure 3a, left). Seven surface samples have been  
215 analysed and their calculated  $^{10}\text{Be}$  age distribution is multimodal. Discarding the possible  
216 outlier DS08S114 ( $49.9 \pm 3.3$  ka), their weighted mean  $^{10}\text{Be}$  age is of  $175 \pm 62$  ka (Table 1,  
217 Figure 3a, right). In order to try to better constrain the abandonment age of this alluvial  
218 deposit, seven samples were taken at increasing depths along a 4-m profile. Each sample is an  
219 amalgam of 10-30 pebbles aiming at measuring the mean concentration at each level. The  
220 random evolution of the measured  $^{10}\text{Be}$  concentrations as a function of depth does not permit  
221 to plainly model the obtained depth-profile and hence to define a limiting isochron as  
222 theoretically proposed by Ryerson et al. (2006). This random distribution excludes uniform  
223 pre-exposure of the material, prior to its emplacement as the T2 alluvial terrace, and suggests  
224 thus variable inheritance. Recent work dealt with the occurrence of variable inheritance in  
225 alluvial terraces (e.g., Schmidt et al., 2011). In the latter, a variable inheritance is evidenced  
226 only in boulders collected on the surface while concentration of sand samples decrease  
227 exponentially along a depth-profile, suggesting a homogeneous inheritance. Schmidt et al.  
228 (2011) suggest that the differences in the inherited component are related to the different  
229 provenances and pre-exposure histories of the different material. In our case, the variability of  
230 inheritance is observed for pebbles and cobbles of different nature (quartz for  $^{10}\text{Be}$  and  
231 carbonates for  $^{36}\text{Cl}$ ) for which internally coherent results have been obtained on a same  
232 terrace (Le Dortz et al., 2011). The method described in section 1 was thus used to account for  
233 the variability and derive accurate bounds on the minimum inheritance.

234 The performed analysis indicates that terrace T2 was abandoned at most 107 ka ago,  
235 that is the time required to bring sample P127 concentration back from its current value to  
236 zero without bringing back any other depth-profile sample to a negative concentration (Figure  
237 3b). The concentration in excess remaining after subtracting to the measured concentration  
238 the concentration accumulated by *in-situ* production during 107 ka at the sampling depth

239 corresponds for all samples but P127 to the decay of the original inherited component (Table  
240 A.1). Concentration in excess are ranging from  $2.15 \times 10^5$  at/g( $\text{SiO}_2$ ) (sample P126) to  
241  $7.86 \times 10^5$  at/g( $\text{SiO}_2$ ) (sample P130). After correcting for the radioactive decay during the last  
242 107 ka, the inherited concentrations corresponding to the maximum abandonment age of the  
243 T2 terrace (Table A.1) are ranging from  $2.27 \times 10^5$  to  $8.29 \times 10^5$  at/g( $\text{SiO}_2$ ). As mentioned  
244 previously, one has to demonstrate that the depth-profile samples and the surface samples  
245 originated from the same source area. As discussed above, summing the surface concentration  
246 accumulated during 107 ka exposure duration to each concentration in excess determined for  
247 the depth samples (see Appendix and Table A.1) yields to depth-profile derived surface  
248 concentrations within the range of those measured in the surface samples (Figure A.1).

249 Moreover, the other possible abandonment ages based either on the lowest surface  
250 concentration (minimum cosmogenic nuclide abandonment age of 50 ka) or even on the OSL  
251 ages ( $\approx 30$ ka) yield similar conclusions. Thus, all these statistical considerations demonstrate  
252 *a posteriori* that the gravels of the depth-profile and the ones of the fan surface sample  
253 originate from the same variably pre-exposed source and can thus be compared. Regarding  
254 the surface samples, the profile rejuvenation method using the concentration accumulated at  
255 the surface by *in-situ* production during 107 ka brings only one of the surface samples to a  
256 negative concentration (Figure, 3b). This remains acceptable as this sample is, in addition, the  
257 statistical outlier DS08S114. It is nonetheless important to notice that this age of 107 ka is the  
258 uppermost bound for the abandonment age and thus for the *in situ* exposure duration.  
259 Consequently, exposure ages ranging from 0 to 107 ka are theoretically possible for the T2  
260 surface. On the one hand, exposure ages ranging between 53 ka (oldest possible age of the  
261 youngest sample, DS08S114, Table 1) and 107 ka would make that statistical outlier younger  
262 than the age of the terrace. On the other hand, exposure ages ranging between zero and 53 ka  
263 would be compatible with the occurrence of the statistical outlier as well as the other surface  
264 samples collected on T2. All exposure ages younger than 47 ka (youngest possible age of the  
265 youngest sample, DS08S114, Table 1) would imply that the youngest sample collected at the  
266 surface has a significant inherited component. At this location, two OSL ages yielded  
267  $26.9 \pm 1.3$  ka at 0.8 m depth and  $29.4 \pm 5.1$  ka at 3.4 m depth, suggesting that the terrace  
268 material aggraded on a short period of time and that the youngest CRE sample may still  
269 contain some inheritance.

270 Because surface sampling does not allow accounting for inheritance, while profile  
271 rejuvenation permits retrieving the range of variable inheritance, the age range of  $175 \pm 62$  ka  
272 obtained considering the sole surface samples is incompatible with the maximum cosmogenic

273 nuclide abandonment age deduced from the depth profile samples analysis. As a consequence,  
274 the lowest surface concentration (DS08S114, Table 1) measured in the statistical outlier,  
275 provides a realistic minimum cosmogenic nuclide abandonment age of  $50 \pm 3$  ka. This T2  
276 minimum abandonment age yields to maximum inheritance ranging between  $3.29 \times 10^5$  and  
277  $8.59 \times 10^5$  at/g (Figure 3c and Table A.1). Selecting a youngest abandonment age derived from  
278 the OSL ages would increase very slightly the inheritance without changing the overall figure  
279 (see Table A.1).

280 Therefore, the cosmogenic nuclide abandonment ages range for T2 abandonment  
281 should be narrowed to 47-107 ka and the alluvial material appears to have emplaced with  
282 inherited concentrations ranging from  $2.27 \times 10^5$  to  $8.7 \times 10^5$  at/g.

283

284

### 285 3. Case study

#### 286 3.1 Example of an old terrace

287 In the same region (Figure 4a, left), the  $^{10}\text{Be}$  concentrations measured along a depth-  
288 profile from a higher, hence older, terrace (T3; see Le Dortz et al., 2011) were analysed. The  
289 *in-situ* produced  $^{10}\text{Be}$  concentrations increasing with the exposure duration and the  $^{10}\text{Be}$   
290 inherited concentrations radioactively decreasing, it can be anticipated that the proportion of  
291 *in-situ* produced  $^{10}\text{Be}$  with respect to the inherited one increases with the abandonment age.  
292 The longer is the *in-situ* exposure duration, the higher is the dilution of inheritance. Ten  
293 quartz samples were collected on the T3 tread (Table 1 and Figure 4a, right). The distribution  
294 of these surface CRE ages, considering sample DN06S2 ( $235.5 \pm 35.4$ ) as an outlier, is  
295 unimodal and leads to a weighted mean CRE age of  $462 \pm 55$  ka. Amalgamated samples have  
296 also been collected along a depth-profile. Their  $^{10}\text{Be}$  concentrations exhibit an overall  
297 exponential decrease with depth but the deepest sample displays nonetheless a much higher  
298 concentration than the two samples above it. Such a  $^{10}\text{Be}$  depth-profile can theoretically be  
299 modelled (pink curve, Figure 4b). The best fit, assuming no denudation, is obtained for an  
300 abandonment age of 464 ka and a homogeneous inheritance of  $3.8 \times 10^5$  at/g ( $\text{SiO}_2$ ), which  
301 would correspond to a pre-exposure duration of  $\sim 32$  ka, if acquired at the surface in  
302 conditions similar to that at the Dehshir North site (Le Dortz et al., 2011). One may find  
303 satisfactory the coherence between the abandonment ages deduced from the surface samples  
304 and the modelling of the depth-profile samples. However, the fact that the inherited  
305 concentration derived from the modelling of the depth-profile is half the concentrations  
306 measured for the deepest samples is intriguing, and opens the possibility for the occurrence of

307 variable inheritance. As for T2, the methodology described to estimate the minimum  
308 inheritance considering only the depth-profile samples has thus been applied to T3.

309 For T3, the depth-profile sample, whose concentration can be restored to zero by  
310 subtracting a simple *in-situ* exposure duration at the sampling depth without bringing back  
311 any other depth-profile sample to a negative concentration, is P12 (Figure 4b and Table A.1).  
312 The minimum excess concentration ( $2.43 \times 10^5$  at/g ( $\text{SiO}_2$ )) is obtained for sample P17,  
313 collected at 2.7 m depth, and the maximum excess concentration ( $9.04 \times 10^5$  at/g ( $\text{SiO}_2$ )) is  
314 obtained for sample P14. Accounting for the radioactive decay, this brackets the minimum  
315 inherited component between  $2.99 \times 10^5$  and  $11.1 \times 10^5$  at/g.

316 The maximum cosmogenic nuclide abandonment age of 412 ka deduced from the  
317 profile rejuvenation method agrees with the range of abandonment ages deduced from surface  
318 samples only ( $462 \pm 55$  ka). This consistency is significant when considering that summing  
319 the surface concentration accumulated during 412 ka exposure duration to each concentration  
320 in excess determined for the depth samples yields to depth profile derived surface  
321 concentrations within the range of those measured in the surface samples (see Appendix,  
322 Figure A.2 and Table A.1). This allows narrowing the abandonment age interval to 407-412  
323 ka. It is worth noticing that this rejuvenation would yield only one of the surface samples to a  
324 negative concentration, the statistical outlier DN06S2 (Figure 4b). All the other such  
325 rejuvenated surface samples display positive excess concentrations. While abandonment ages  
326 for the terrace T3 older than 412 ka are not possible because they would imply a negative  
327 concentration for at least one depth-profile amalgam (P12), younger exposure ages remain  
328 possible. Theoretically, all exposure ages ranging between 0 and 412 ka are possible. On the  
329 one hand, exposure ages ranging between 271 ka (oldest possible age of the youngest T3  
330 surface sample DN06S2, Table 1) and 412 ka would make that statistical outlier younger than  
331 the age of the terrace. On the other hand, exposure ages ranging between zero and 200 ka  
332 (youngest possible age of the youngest T3 sample DN06S2, Table 1) would be compatible  
333 with the occurrence of the statistical outlier as well as the other surface samples collected on  
334 T3. All ages younger than 200 ka would imply that the youngest surface sample also contains  
335 some inheritance.

336 One may therefore consider the youngest surface sample -i.e., the statistical outlier  
337 DN06S2 ( $235.55 \pm 35.38$  ka) - as the last pebble emplaced on the T3 tread before its  
338 abandonment and subsequent incision. Considering the possibility for a variable inheritance  
339 as for T2, the age of sample DN06S2 might be closer to the abandonment age of surface T3.  
340 If the concentration corresponding to 235 ka of *in-situ* production at their sampling depth is

341 subtracted to each surface and depth-profile sample, the age distribution of such rejuvenated  
342 surface samples remains unimodal (Figure 4c, top). However the concentrations of the  
343 “rejuvenated” depth-profile samples remain too scattered to allow for a simple profile  
344 modelling, revealing that inheritance is not homogeneous (Figure 4c, bottom). The minimum  
345 abandonment age of 235 ka, which is calculated for T3, permits to estimate the range of the  
346 variable maximum inheritance. Accounting for the radioactive decay, the range of the  
347 maximum inheritance between  $3.62 \times 10^5$  and  $16.12 \times 10^5$  at/g appears rather large (Table A.1).  
348 This case study illustrates that an unknown and variable inheritance can always be modelled  
349 as a homogeneous inheritance once the portion of the concentration that has been acquired at  
350 the sampling depth since the deposit emplacement becomes significantly larger than that  
351 inherited from surface pre-exposure.

352

### 353 ***3.2 Example of a young terrace***

354 A similar approach has been applied to the surface and depth-profile samples of a young  
355 terrace level (the T1 terrace offset by the Anar fault along the western piedmont of the Kuh-e-  
356 Bafq about 150 km east of the Dehshir sites, Figure 5a, left; see Le Dortz et al., 2009). For a  
357 young terrace, the proportion of inherited concentration, if there is any, may be large with  
358 respect to the *in-situ* produced concentration acquired at the sampling depth since the deposit  
359 emplacement. Ten quartz samples and seven amalgamated samples were collected on the  
360 surface and along a depth-profile through a well-defined abandoned fan surface, respectively  
361 (figure 5). The CRE ages of the surface samples are scattered and display a multimodal  
362 distribution with a weighted mean CRE age of  $32 \pm 25$  ka (Figure 5a, right). This terrace  
363 appears significantly younger than the ones studied in the Dehshir area. The error-bars on the  
364 mean value are too large to allow tightly constraining an abandonment age. The distribution  
365 of depth-profile concentrations is random, dismissing a homogeneous pre-exposure prior to  
366 the emplacement of the fan material (Figure 5b). Besides, the deepest depth-profile samples  
367 display  $^{10}\text{Be}$  concentrations larger than that of many of the surface samples. This exemplifies  
368 the occurrence of a variable inheritance and led Le Dortz et al. (2009) to approximate the  
369 abandonment age of the terrace by that of the youngest pebble.

370 Applying the rejuvenation method described above to the depth-profile samples yields  
371 a maximum cosmogenic nuclide abandonment age of 46 ka, which implies minimum excess  
372 concentrations ranging from  $0.7 \times 10^5$  to  $4.16 \times 10^5$  at/g ( $\text{SiO}_2$ ) (Figure 5b and Table A.1).  
373 Summing the surface concentration accumulated during 46 ka exposure duration to each  
374 concentration in excess determined for the depth samples indeed yields to depth-profile

375 derived surface concentrations that are not fully compatible with those measured in the  
376 surface samples (see Appendix, Table A.1 and Figure A.3). In addition, applying this  
377 maximum cosmogenic nuclide abandonment on surface samples implies that all but one of the  
378 rejuvenated surface samples would display negative concentrations, highlighting that the  
379 maximum cosmogenic nuclide abandonment age of 46 ka deduced from the rejuvenation of  
380 the depth-profile data is largely overestimating the actual abandonment age of the terrace.  
381 Minimum inheritance must then be higher than those estimated using the profile rejuvenation  
382 method, which prevents determining a maximum cosmogenic nuclide age. The abandonment  
383 age of the alluvial surface is thus better approximated by the CRE age of the youngest surface  
384 sample ( $17.5 \pm 1.1$  ka; sample AS06S75 in Table 1). Subtracting a concentration  
385 corresponding to a simple exposure duration of 17.5 ka at their sampling depth, one verifies  
386 that none of the depth-profile sample has been emplaced with a negative concentration  
387 (Figure 5c). This minimum CRE age of 17.5 ka permits to calculate a range of maximum  
388 inheritance bracketed between  $1.48 \times 10^5$  and  $4.30 \times 10^5$  at/g ( $\text{SiO}_2$ ). This confirms that the  $^{10}\text{Be}$   
389 concentration of the deepest sample (P97) results nearly entirely from inheritance whatever  
390 the range of theoretical exposure age (0-46 ka). It is nonetheless possible that the youngest  
391 surface sample concentration also incorporates some inheritance. This is the case for this  
392 studied Anar site as demonstrated by OSL burial ages associated to samples collected below  
393 the tread ( $5.8 \pm 3.6$  ka at 0.8 m depth and  $14.4 \pm 3.9$  ka at 4.1 m depth) that are younger than the  
394 CRE ages of pebbles collected on the tread (Le Dortz et al., 2009). Interestingly summing the  
395 surface concentration accumulated during either 17.5 ka (youngest CRE age) or 10 ka  
396 (average OSL age of the final fan aggradation) exposure duration to each corresponding  
397 concentration in excess determined for the depth samples yields to depth profile derived  
398 surface concentrations that are compatible with those measured in the T1 surface samples (see  
399 Appendix, Table A.1 and Figure A.3). This again demonstrates that the depth-profile and  
400 surface samples originate from the same source. Therefore, this case study illustrates the  
401 limitation of the profile rejuvenation method for very young alluvial surfaces (0-20 ka) for  
402 which, the portion of variable inheritance is significant with respect to the proportion of the  
403 concentration acquired at the sampling depth since the deposit emplacement. In such  
404 conditions, it appears more pertinent to rely on the youngest surface sample to approximate  
405 the age of the surface.

406

407

408 **Conclusion**

409           The profile rejuvenation method allows handling the complications raised by variable  
410 inheritance when using *in-situ* produced cosmogenic nuclide concentrations in regions where  
411 denudation is demonstrated negligible, a necessary condition which limits the unknowns to  
412 the *in-situ* exposure duration and to the inherited component resulting from pre-exposure.  
413 This approach is illustrated by analyses of samples collected from alluvial terraces in the arid  
414 environment of the central Iran plateau where denudation has been demonstrated negligible  
415 (Le Dortz et al., 2011). Where depth-profiles cannot be modelled to determine a  
416 homogeneous inheritance, this profile rejuvenation procedure may allow to derive from the  
417 depth-profile samples a maximum cosmogenic nuclide abandonment age for the surface of an  
418 alluvial terrace and to estimate a range of minimum inherited concentrations. The consistency  
419 between the surface and depth profile concentrations has to be checked for each site to ensure  
420 that both surface and depth profile samples originate from the same source (see Appendix).  
421 When the profile rejuvenation method yields negative concentrations for most of the surface  
422 samples, this indicates that the profile derived maximum abandonment age significantly  
423 overestimates the actual surface abandonment age. As a consequence, the youngest of the  
424 surface samples appears as the best approximation for the abandonment age of the alluvial  
425 terrace rather than the weighted mean CRE age of many samples. This youngest age provides  
426 the minimum abandonment age based on CRE data and permits to calculate a range of  
427 maximum inheritance. Interestingly, this was empirically formulated for Holocene terraces at  
428 some places in Mongolia (Vassallo et al., 2007) and at some sites along the southern rim of  
429 the Tarim basin (Mériaux et al., 2005). The different sites we analyzed in the desert  
430 environment of central Iran show that the procedure of rejuvenation profile allows handling  
431 the variable inheritance of alluvial material whatever the age of the analyzed terrace. In  
432 central Iran, where variable inheritance is observed, the inherited concentrations range  
433 between  $1.48 \times 10^5$  and  $16.1 \times 10^5$  at/g. However, the range of inheritance for a given site is  
434 much smaller, the inheritance concentrations varying approximately in a ratio 1-3. In addition,  
435 the maximum inheritance values appear to increase with terrace abandonment ages.  
436 Nevertheless, we do not have enough sites to ascertain such conclusion and this observation  
437 may only reflect difference in catchments and/or in pre-exposure processes. If the observed  
438 inheritances would have accumulated at the surface, they would be equivalent to CRE  
439 duration ranging from 15 ka to 130 ka.

440           The occurrence of such high, inherited concentrations for the sites analyzed in central  
441 Iran may result from the endorheic drainage of the Iranian plateau that prevents significant  
442 fluvial incision (Le Dortz et al., 2009). Thus, low denudation rates and weak incision favour

443 the feeding of alluvial fans or terraces by reworking older alluvial material. As a consequence,  
444 this older alluvial material has been previously exposed to cosmic rays and carries a variable  
445 amount of inheritance according to the depth where it was eroded and/or the number of times  
446 it was reworked. This alluvial "cannibalism" may also characterize many arid endorheic  
447 regions such as Altiplano, central Asia (Tarim, Mongolia, Tibet...), where the amount of  
448 denudation is thought negligible. Therefore, this method could be usefully applied to analyze  
449 the cosmogenic nuclide concentrations in such regions to determine bounds of maximum *in-*  
450 *situ* CRE duration and ranges of inheritance.

451 Even more interesting than the important amount of inheritance is the high variability  
452 of that inheritance expressed by the random distribution of the concentrations of the  
453 amalgams along a given profile. Indeed, smaller variations between two successive samples  
454 amalgamating 10-30 pebbles at a given depth are expected, anticipating they average the  
455 cosmogenic nuclide concentrations at that depth. The variability among amalgams may thus  
456 represent sudden and uneven episodes of aggradation of material exhumed from different  
457 places of the upper catchments. This would explain a rapid aggradation of the fanglomerates  
458 together with the lack for exponential decrease of the concentrations with depth. These  
459 observations may result from the fact the cosmogenic nuclide concentrations, which built up  
460 in landscape, are not completely reset by erosional climatic crisis. As a consequence, OSL  
461 ages may help constraining the history of alluvial aggradation (e.g., Le Dortz et al., 2009 and  
462 2011; Fruchter et al., 2011; Guralnik et al, 2011). Finally, this study demonstrates the  
463 usefulness of combining both surface and depth-profile sampling either to approach  
464 confidently the abandonment age of alluvial fans or to document their aggradation history.

465  
466

#### 467 **Acknowledgments:**

468 This study benefited from initial funding by PNTS and 3F INSU programs. Université Pierre  
469 et Marie Curie (UPMC) and Geological survey of Iran (GSI) provided the complementary  
470 funding and the logistic assistance. KL received a Ministry of Research and Education  
471 scholarship granted by the President of UPMC. The  $^{10}\text{Be}$  measurements were performed at  
472 the ASTER AMS national facility (CEREGE, Aix en Provence) that is supported by the  
473 INSU/CNRS, the French Ministry of Research and Higher Education, IRD, and CEA. L.  
474 Leanni, F. Chauvet, M. Arnold and G. Aumaître are acknowledged for their help during  
475 chemistry and measurements. We acknowledge Ari Matmon and one anonymous reviewer for  
476 constructive remarks that helped to greatly improve our manuscript.

477

478

479 **References**

- 480 Anderson, R.S. ; Repka, J.L. ; Dick, G.S., 1996. Explicit treatment of inheritance in dating  
481 depositional surfaces using *in-situ*  $^{10}\text{Be}$  and  $^{26}\text{Al}$ ; *Geology* 24:47-51
- 482 Braucher, R., P. Del Castillo, L. Siame , A.J. Hidy , D.L. Bourlès., 2009. Determination of  
483 both exposure time and denudation rate from an *in-situ*-produced  $^{10}\text{Be}$  depth profile :  
484 A mathematical proof of uniqueness. Model sensitivity and applications to natural  
485 cases. *Quaternary Geochronology* Volume 4, Issue 1, Pages 1-82
- 486 Brown, E.T., Molnar, P., and Bourlès D.L., 2005. Comment on "Slip-Rate Measurements on  
487 the Karakorum Fault May Imply Secular Variations in Fault Motion" *Science* 309  
488 (5739), 1326b. [DOI: 10.1126/science.1112508].
- 489 Champagnac, J.-D., D.-Y. Yuan, W.-P. Ge, P. Molnar, and W.-J. Zheng., 2010. Slip rate at  
490 the northeastern front of the Qilian Shan, China, *Terra Nova*, 22, 180-187.
- 491 Chmeleff, J., von Blackenburg, F., Kossert, K., Jakob, D., 2010. Determination of the  $^{10}\text{Be}$   
492 half-life by multicollector ICP-MS and liquid scintillation counting. *Nuclear*  
493 *Instruments and Methods in Physics Research B*, **268**, 192–199.
- 494 Frankel, K.L., Dolan, J.F., Owen, L.A., Ganev, P.N., and Finkel, R.C., 2011, Spatial and  
495 temporal constancy of seismic strain release along an evolving segment of the  
496 Pacific-North America plate boundary: *Earth and Planetary Science Letters*,  
497 doi:10.1016/j.epsl.2011.02.034
- 498 Fruchter, N., Matmon, A., Avni, Y., Fink, D., 2011. Revealing sediment sources, mixing, and  
499 transport during erosional crater evolution in the hyperarid Negev Desert, Israel.  
500 *Geomorphology* 134, 363–377
- 501 Gosse, J.C., and Phillips, F.M., 2001, Terrestrial in-situ cosmogenic nuclides: theory and  
502 application:. *Quaternary Science Reviews*, v. 20, p. 1475-1560
- 503 Guralnik, B., Matmon, A., Avni, Y., Porat, N., Fink, D., 2011. Constraining the evolution of  
504 river terraces with integrated OSL and cosmogenic nuclide data. *Quat. Geochron.* 6,  
505 22–32.
- 506 Korschinek, G., Bergmaier, A., Faestermann, T., Gerstmann, U. C., Knie, K., Rugel, G.,  
507 Wallner, A., Dillmann, I., Dollinger, G., Lierse von Gosstomski, Ch., Kossert, K.,  
508 Maiti, M., Poutivtsev, M., Rimmert, A., 2010. A new value for the  $^{10}\text{Be}$  half-life by  
509 Heavy-Ion Elastic Recoil detection and liquid scintillation counting. *Nuclear*  
510 *Instruments and Methods in Physics Research B*, **268**, 187–191.

- 511 Le Dortz, K. Meyer B., Sébrier M., Nazari H., Braucher R., Fattahi M., Benedetti L.,  
 512 Foroutan M., Siame L., Bourles D., Talebian M., Bateman M.D. and Ghoraishi M.,  
 513 2009. Holocene right-slip rate determined by cosmogenic and OSL dating on the Anar  
 514 fault, Central Iran. *Geophysical Journal International*, **179**, 700–710, doi :  
 515 10.1111/j.1365-246X.2009.04309.x
- 516 Le Dortz, K. Meyer B., Sébrier M., Braucher R., Nazari H., Benedetti L., Fattahi M., Bourles  
 517 D., Foroutan M., Siame L., Rashidi, A., Bateman M.D., 2011. Dating inset terraces and  
 518 offset fans along the Dehshir fault combining cosmogenic and OSL methods.  
 519 *Geophysical Journal International*, 185, 1147-1174, DOI: 10.1111/j.1365-  
 520 246X.2011.05010.x
- 521 Matmon, A., Schwartz, D.P., Finkel, R., Clemmens, S., Hanks, T., 2005. Dating offset fans  
 522 along the Mojave section of the San Andreas fault using cosmogenic  $^{26}\text{Al}$  and  $^{10}\text{Be}$ .  
 523 *Geol. Soc. Am. Bull.* 117, 795–807.
- 524 Mériaux, A.-S., Tapponnier, P. Ryerson, F. J. Xiwei, X. King, G. Van der Woerd, J. Finkel,  
 525 R. C. Haibing, L. Caffee, M. W. Zhiqin, X., 2005. The Aksay segment of the northern  
 526 Altyn Tagh fault: Tectonic geomorphology, landscape evolution, and Holocene slip  
 527 rate, *J. Geophys. Res.*, **110**, B04404
- 528 Nissen, E., Walker R.T., Bayasgalan B., Carter A, Fattahi M., Molor E., Schnabel C., West A.  
 529 J., Xu S., 2009. The late Quaternary slip-rate of the Har-Us-Nuur fault (Mongolian  
 530 Altai) from cosmogenic  $^{10}\text{Be}$  and luminescence dating, *Earth Planet. Sci. Lett.* 286,  
 531 467-478, doi:10.1016/j.epsl.2009.06.048
- 532 Owen, L.A., Frankel, K.L., Knott, J.R., Reynhout, S., Finkel, R.C., Dolan, J.F., Lee, J., 2011.  
 533 Beryllium-10 terrestrial cosmogenic nuclide surface exposure dating of Quaternary  
 534 landforms in Death Valley. *Geomorphology* 125, 541–557  
 535 doi:10.1016/j.geomorph.2010.10.024.
- 536 Regard, V., O. Bellier, R. Braucher, F. Gasse, D. Bourlès, J. Mercier, J.-C. Thomas, M.R.  
 537 Abbassi, E. Shabaniyan and Sh. Soleymani, 2006.  $^{10}\text{Be}$  dating of alluvial deposits from  
 538 Southeastern Iran (the Hormoz Strait area), *Palaeogeography, Palaeoclimatology,*  
 539 *Palaeoecology*, 242, 36-53.
- 540 Repka, J. L., R. S. Anderson and R. C. Finkel, 1997. Cosmogenic dating of fluvial terraces,  
 541 Fremont River, Utah; *Earth and Planetary Science Letters* 152:59-73
- 542 Ritz, J.F., Brown, E.T., Bourlès, D.L., Philip, H., Schlupp, A., Raisbeck, G.M., Yiou, F., and  
 543 Enkhtuvshin, B. 1995. Slip rates along active faults estimated with cosmic-ray-exposure  
 544 dates: Application to the Bogd fault, Gobi- Altaï, Mongolia. *Geology* 23: 1019-1022.

- 545 Ryerson, F.J., Tapponnier, P., Finkel, R.C., Meriaux, A., Van der Woerd, J., Lasserre, C.,  
546 Chevalier, M., Xiwei, X., Haibing, L., King, G.P., 2006. Applications of  
547 morphochronology to the active tectonics of Tibet. *GSA, Special Papers*, **415**, 61-86,  
548 doi: 10.1130/2006.2415(05)
- 549 Schmidt, S., Hetzel, R., Kuhlmann, J., Mingorance, F., Ramos, V.A., 2011. A note of caution  
550 on the use of boulders for exposure dating of depositional surfaces. *Earth and*  
551 *Planetary Science Letters*, **302**, 60-70. doi: 10.1016/j.epsl.2010.11.039.
- 552 Siame, L., O. Bellier, R. Braucher, M. Sebrier, M. Cushing, D. Bourlès, B. Hamelin, E.  
553 Baroux, B. de Voogd, G. Raisbeck, F. Yiou, 2004. Local erosion rates versus active  
554 tectonics : cosmic ray exposure modelling in Provence (south-east France). *Earth*  
555 *Planet. Sci. Lett*, **220**, 3-4, 345-364.
- 556 Stone J. O., 2000. Air pressure and cosmogenic isotope production. *J. Geophys. Res.*,105,  
557 B10, 23753-23759.
- 558 Van der Woerd, J., F. J. Ryerson, P. Tapponnier, Y. Gaudemer, R. C. Finkel, A.-S. Meriaux,  
559 M. W. Caffee, G. Zhao, and Q. He, 1998. Holocene left slip-rate determined by  
560 cosmogenic surface dating on the Xidatan segment of the Kunlun fault (Qinghai,  
561 China), *Geology* 26,695 –698.
- 562 Van der Woerd, J., Klinger Y., Sieh K., Tapponnier P., Ryerson F.J., Mériaux A-S., 2006.  
563 Long-term slip rate of the southern San Andreas fault from 10Be-26Al surface exposure  
564 datation of an offset alluvial fan, *J. Geophys. Res.*, 111, B04407.
- 565 Vassallo R, Ritz J, F., Braucher R, Jolivet M, Carretier S, Larroque C, Chauvet A, C. Sue C,  
566 Todbileg M, Bourlès D, Arzhannikova A, Arzhannikov S., 2007. Transpressional  
567 tectonics and stream terraces of the Gobi-Altay, Mongolia. *Tectonics* 26, TC5013,  
568 doi:10.1029/2006TC002081.
- 569 Vermeesch, P., 2007. CosmoCalc: An Excel add-in for cosmogenic nuclide calculations,  
570 *Geochem. Geophys. Geosyst.*, **8**, Q08003, doi:10.1029/2006GC001530.

571 ***Appendix: Comparison of depth-profile concentrations with surface concentrations***

572

573 The comparison between surface concentrations and depth-profile concentrations  
574 cannot be performed directly because cosmogenic nuclide production rate is extremely  
575 sensitive to depth. Theoretically, concentrations only resulting from accumulation at any  
576 depth below the surface (i.e., *in-situ* production with no denudation and no inheritance) may  
577 be converted to concentrations the samples would have accumulated at the surface during the  
578 same exposure duration using the inverse function of neutron attenuation. However,  
579 concerning the analyzed Iranian sites, where scattering of both depth-profile and surface  
580 concentrations is observed within alluvial material, this depth to surface conversion cannot be  
581 achieved *a priori* because the measured concentrations are the result of two unknown  
582 components: the *in-situ* exposure duration and the variable inheritance. Consequently, it is  
583 only possible to perform an *a posteriori* comparison, which relies on the estimated  
584 abandonment ages of an analyzed alluvial surface. For each abandonment age, the  
585 corresponding *in-situ* contribution may be calculated for any depth-profile sample.  
586 Subtracting this calculated *in-situ* contribution from the measured concentration yields the  
587 current excess concentration of a given depth-profile sample. Then, adding this current excess  
588 concentration to the *in-situ* concentration accumulated at the surface, during an exposure  
589 duration corresponding to the abandonment age, yields to the concentration that the depth-  
590 profile samples would have if emplaced and remaining at the surface. Performing such  
591 concentration conversion for all the samples of a depth-profile allows comparing depth-  
592 profile samples to surface samples.

593 Table A.1 provides all the measured cosmogenic nuclide concentrations and all the  
594 results of the calculation that have been performed to convert depth-profile concentrations to  
595 surface ones. For each analyzed site, these concentration conversions have been made at least  
596 for two exposure durations: (1) the maximum abandonment age ( $t_{\text{Max}}$ ), which has been  
597 determined by the profile rejuvenation method (see section 2 and 3), and (2) the minimum  
598 abandonment age ( $t_{\text{min}}$ ), calculated from the lowest surface concentration. When OSL ages  
599 were available, they have also been used to perform a depth to surface conversion. In  
600 addition, a last column provides the inherited concentration at the time of alluvial aggradation  
601 (i.e., the inheritance resulting from pre-exposure). It corresponds to the current excess  
602 concentration corrected for radioactive decay.

603 Three figures illustrate the distribution of the measured surface concentrations and of  
604 the differently converted depth-profile concentrations to surface ones. These figures are

605 presented in the same order as the sites analyzed in the text. Concerning the site of T2 terrace  
606 (see section 2), three abandonment ages are considered: 107 ka ( $t_{\text{Max}}$ ), 50ka ( $t_{\text{min}}$ ), and 30 ka  
607 ( $t_{\text{OSL}}$ ). All the converted depth-profile concentrations, calculated using these abandonment  
608 ages are compared to the surface concentrations (Figure A.1 and Table A.1). This comparison  
609 indicates that the depth-profile and surface samples originate from the same source. Thus,  
610 they can be compared and analyzed jointly. Nevertheless, it appears that the converted depth-  
611 profile concentrations systematically exhibit a narrower range of values than the surface  
612 concentrations. This should be the consequence of the sampling amalgamation that tends to  
613 average the actual sample variability. The converted depth-profile concentrations decrease  
614 with the abandonment ages. Nevertheless, while the *in-situ* contribution decreases with the  
615 abandonment age, inheritance remains comparable within the range  $\approx 3$  to  $8.5 \times 10^5$  at/g. For  
616 the T3 site (section 3.1), only two abandonment ages may be considered. All the converted  
617 depth-profile concentrations, calculated using both cosmogenic nuclide abandonment ages are  
618 compared to the measured surface concentrations (Figure A.2 and Table A.1). However, the  
619 two abandonment cosmogenic nuclide ages yield significant differences as the two possible  
620 ranges of converted concentrations do not nearly overlap. The depth-profile concentrations  
621 converted using 412 ka ( $t_{\text{Max}}$ ) are within the range of the measured surface concentrations that  
622 defines the Gaussian distribution (see figure 4a, right) while those converted using 235 ka  
623 ( $t_{\text{min}}$ ) lie between the Gaussian distribution of the measured surface concentrations and the  
624 measured lowest surface concentration. Depending on whether the lowest surface  
625 concentration is interpreted as the best  $t_{\text{min}}$  approximation or as an outlier, this solution may  
626 be considered as valid or not. Whatever the choice, as mentioned in section 3.1, the solution  
627 based on 412 ka provides a significantly higher value for the maximum inheritance than the  
628 mean determined by profile modelling (see Figure 4b and Table A.1). Concerning the T1  
629 terrace site (see section 3.2), three abandonment ages are considered: 46 ka ( $t_{\text{Max}}$ ), 17.5 ka  
630 ( $t_{\text{min}}$ ), and 10 ka ( $t_{\text{OSL}}$ ). All but the one based on 46 ka of the converted depth-profile  
631 concentrations are within the range of the surface concentrations (Figure A.3 and Table A.1).  
632 However, it is noteworthy to stress that the results obtained considering  $t_{\text{Max}}$  are inconsistent  
633 with the T1 surface data. Then, this maximum cosmogenic nuclide abandonment age is most  
634 likely unrealistic. Considering the two younger abandonment ages of 17.5 ka and 10 ka, the  
635 obtained converted concentrations are compared with the measured surface concentrations  
636 (Figure A.3). As for the T2 site, they appear to determine a narrower range of values than the  
637 surface concentrations. At this site, the range of inheritance, from  $\sim 1.5$  to  $4.5 \times 10^5$  at/g, also  
638 remains approximately stable even if the abandonment age decreases.

639           Therefore, the comparison between the depth-profile and the surface concentrations,  
640   which can be realized *a posteriori*, indicates that all the alluvial samples originate from the  
641   same variably pre-exposed source. As a consequence, depth-profile and surface samples can  
642   be analyzed jointly.

ACCEPTED MANUSCRIPT

643

644 **Figure captions**

645

646 Figure 1: Usual strategies of surface and depth-profile sampling for determining exposure age  
647 of alluvial surfaces. a) Individual quartz pebbles are collected for surface sampling while  
648 amalgams of 10-30 centimetre-sized pebbles are used for depth-profile sampling. b) Surface  
649 exposure age determination using (top) weighted mean  $^{10}\text{Be}$  CRE age for surface samples and  
650 (bottom) modelling an exponential decrease of the concentrations with depth for depth-profile  
651 samples. Blue and black samples for theoretical cases, dark pink and light pink domains  
652 figure out the *in-situ* production acquired with and without homogeneous inheritance,  
653 respectively. With homogeneous inheritance, the Gaussian distribution of the surface samples  
654 is shifted providing an artificial CRE age older than the current age of surface abandonment.  
655 The shift corresponds to the inherited  $^{10}\text{Be}$  concentration that the modelling of a depth-profile  
656 may evidence. The homogeneous inheritance is the concentration value toward which the  
657 modelled profile asymptotically tends. c) With a variable inheritance, CRE surface ages are  
658 often scattered and their distribution is multimodal. There is no exponential decrease of the  
659 concentrations with depth making helpless any profile modelling (dashed curve).

660

661 Figure 2 : Illustration of the rejuvenation method. a) Red dots are the concentrations measured  
662 for the depth-profile amalgams and the surface samples. If there is no denudation, then the  
663 scatter of concentrations results only from a variable inheritance. b) The first step requires  
664 calculating the time needed for one of the depth-profile samples to be brought back to a null  
665 concentration without bringing the other samples to a negative concentration. The  
666 concentration of that sample is indicated in red while the theoretical *in-situ* concentration  
667 expected at the depth of the other profile samples is indicated by blue dots. The *in-situ*  
668 exposure duration required to bring that depth-profile sample to its measured concentration  
669 corresponds to the maximum abandonment age ( $t_{\text{Max}}$ ) of the terrace and is indicated in red  
670 with the pink domain figuring the corresponding *in-situ* production. The blue arrows indicate  
671 the excess concentrations remaining in the other depth-profile samples. c) The second step  
672 consists in comparing these rejuvenated profile concentrations with the rejuvenated surface  
673 samples (blue dots with error bars). If the profile rejuvenation shifts most of the surface  
674 concentrations to positive values (left panel), then the calculated abandonment age provides a  
675 maximum possible age for the surface. On the other hand, if most of the rejuvenated surface  
676 concentrations are shifted to negative values (right panel), there is inconsistency and the

677 calculated abandonment age overestimates the actual age of the surface. d) A third step allows  
 678 calculating a minimum abandonment age ( $t_{\min}$ ). Green dots are the concentrations obtained for  
 679 the depth-profile amalgams and for the surface samples once rejuvenated by the age of *in-situ*  
 680 exposure of the youngest surface sample at their sampling depth, assuming this youngest  
 681 sample on the surface best approximates its age of abandonment.

682

683 Figure 3: a) Inset is a simplified tectonic map of central and eastern Iran with major active  
 684 faults indicated. Black dot indicates site of sampling. On the right, surface age distribution of  
 685 the alluvial terrace T2 at the Dehshir South site. Weighted mean  $^{10}\text{Be}$  CRE ages of the terrace  
 686 tread samples are indicated in red and in blue for the rejuvenated surface samples (for  $t_{\text{Max}}$ ,  
 687 see b). The thin curves represent the CRE age probability as Gaussian distribution for each  
 688 individual sample and the thick curves correspond to the summed Gaussian density  
 689 probability function. The uncertainties associated to the weighted mean age correspond to two  
 690 standard deviations ( $2\sigma$ ). b)  $^{10}\text{Be}$  depth-profile concentrations through the alluvial terrace.  
 691 Red dots are the concentrations measured in the depth-profile amalgams and in the surface  
 692 samples. Blue dots are the concentrations obtained for the depth-profile amalgams and the  
 693 surface samples once one depth-profile amalgam (P127) is restored to a null concentration  
 694 without bringing back any other depth-profile sample to a negative concentration. The time  
 695 ( $t_{\text{Max}}$ ) of *in-situ* exposure to bring that depth-profile sample to its measured concentration is  
 696 indicated in red with the pink domain figuring the corresponding *in-situ* production. The blue  
 697 arrows indicate the excess concentrations remaining in the other depth-profile samples. c)  
 698 Green dots are the concentrations obtained for the depth-profile amalgams and for the surface  
 699 samples once rejuvenated by 50 ka of *in-situ* exposure ( $t_{\min}$ ) at their sampling depth, assuming  
 700 the youngest sample on the surface best approximates its abandonment age. Weighted mean  
 701  $^{10}\text{Be}$  CRE ages of the terrace tread samples are indicated in red and in green once rejuvenated.

702

703 Figure 4: a) Inset is a simplified tectonic map of central and eastern Iran with major active  
 704 faults indicated. Black dot indicates site of sampling. On the right, surface age distribution of  
 705 the alluvial terrace T3 at the Dehshir North site. Weighted mean  $^{10}\text{Be}$  CRE ages of the terrace  
 706 tread samples are indicated in red and in blue for the rejuvenated surface samples (for  $t_{\text{Max}}$ ,  
 707 see b). The thin curves represent the CRE age probability as Gaussian distribution for each  
 708 individual sample and the thick curves correspond to the summed Gaussian density  
 709 probability function. The uncertainties associated to the weighted mean age correspond to two  
 710 standard deviations ( $2\sigma$ ). b)  $^{10}\text{Be}$  depth-profile concentrations through the alluvial terrace.

711 Red dots are the concentrations measured for the depth-profile amalgams and the surface  
712 samples. Blue dots are the concentrations obtained for the depth-profile amalgams and the  
713 surface samples once one depth-profile amalgam (P12) is restored to a null concentration  
714 without bringing back any other depth-profile sample to a negative concentration. The time  
715 ( $t_{\text{Max}}$ ) of *in-situ* exposure to bring that depth-profile sample to its measured concentration is  
716 indicated in red with the pink domain figuring the corresponding *in-situ* production. The blue  
717 arrows indicate the excess concentrations remaining in the other depth-profile samples. The  
718 curve showing the best fit to the depth-profile concentrations is obtained with an age of 464  
719 ka, a homogeneous inheritance of  $3.8 \times 10^5$  at/g ( $\text{SiO}_2$ ), a null denudation rate and a  $\chi^2$  of 931.  
720 c) Green dots are the concentrations obtained for the depth-profile amalgams and for the  
721 surface samples once rejuvenated by 235 ka of *in-situ* exposure duration ( $t_{\text{min}}$ ) at their  
722 sampling depth, assuming the youngest sample on the surface best approximates its age of  
723 abandonment. Weighted mean  $^{10}\text{Be}$  CRE ages of the terrace tread samples are indicated in red  
724 and in green once rejuvenated.

725

726 Figure 5: a) Inset is a simplified tectonic map of central and eastern Iran with major active  
727 faults indicated. Black dot indicates site of sampling. On the right, surface age distribution of  
728 the alluvial terrace T1 at the Anar site. Weighted mean  $^{10}\text{Be}$  CRE ages of the terrace tread  
729 samples are indicated in red and in blue for the rejuvenated surface samples (for  $t_{\text{Max}}$ , see b).  
730 The thin curves represent the CRE age probability as Gaussian distribution for each individual  
731 sample and the thick curves correspond to the summed Gaussian density probability function.  
732 The uncertainties associated to the weighted mean age correspond to two standard deviations  
733 ( $2\sigma$ ). b)  $^{10}\text{Be}$  depth-profile concentrations through the alluvial terrace. Red dots are the  
734 measured concentrations of the depth-profile amalgams and surface samples. Blue dots are  
735 the concentrations obtained for the depth-profile amalgams and surface samples once one  
736 depth-profile amalgam (P102) is restored to a null concentration without bringing back any  
737 other depth-profile sample to a negative concentration. The time ( $t_{\text{Max}}$ ) of *in-situ* exposure to  
738 bring that depth-profile sample to its measured concentration is indicated in red with the pink  
739 domain figuring the corresponding *in-situ* production. The blue arrows indicate the excess  
740 concentrations remaining in the other depth-profile samples. Note that only one of the  
741 rejuvenated surface samples would display a positive concentration (see text for discussion).  
742 c) Green dots are the concentrations obtained for the depth-profile amalgams and for the  
743 surface samples once rejuvenated by 17.5 ka of *in-situ* exposure duration ( $t_{\text{min}}$ ) at their  
744 sampling depth, assuming the youngest sample on the surface best approximates its age of

745 abandonment.

746

747 Figure A.1: a) Distribution of surface  $^{10}\text{Be}$  measured concentration for alluvial terrace T2.  
748  $^{10}\text{Be}$  depth-profile concentrations converted to the surface for abandonment ages of 107 ka  
749 (b), 50 ka (c), and 30 ka (d), respectively (see text of appendix). For each graph the thin  
750 coloured curves represent the concentrations probability as Gaussian distribution for each  
751 individual sample and the thick black curves correspond to the summed Gaussian density  
752 probability function.  
753

754 Figure A.2: a) Distribution of surface  $^{10}\text{Be}$  measured concentration for alluvial terrace T3.  
755  $^{10}\text{Be}$  depth-profile concentrations converted to the surface for abandonment ages of 412 ka (b)  
756 and 235 ka (c), respectively (see text of appendix). For each graph the thin coloured curves  
757 represent the concentrations probability as Gaussian distribution for each individual sample  
758 and the thick black curves correspond to the summed Gaussian density probability function.  
759

760 Figure A.3: a) Distribution of surface  $^{10}\text{Be}$  measured concentration for alluvial terrace T1.  
761  $^{10}\text{Be}$  depth-profile concentrations converted to the surface for abandonment ages of 46 ka (b),  
762 17.5 ka (c), and 10 ka (d), respectively (see text of appendix). For each graph the thin  
763 coloured curves represent the concentrations probability as Gaussian distribution for each  
764 individual sample and the thick black curves correspond to the summed Gaussian density  
765 probability function.  
766

767

768 Table 1: The  $^{10}\text{Be}$  concentrations and CRE modelled ages for surface and depth-profile  
769 samples along the Dehshir and Anar fault. Propagated analytical uncertainties (reported as  $1\sigma$ )  
770 include uncertainties associated with AMS counting statistics, chemical blank measurements  
771 and AMS internal error (0.5%). Zero erosion zero inheritance model ages are calculated for  
772 surface samples taking into account their associated analytical uncertainties, their sampling  
773 geographic coordinates and no shielding, in agreement with site topography. The used  $^{10}\text{Be}$   
774 half-life is 1.387 Ma (Chmeleff et al., 2010; Korschinek et al., 2010). For surface samples, a  
775 density of  $2.2 \text{ g.cm}^{-3}$  has been used for quartz. An attenuation length of  $160 \text{ g.cm}^{-2}$  (Gosse &  
776 Philipps, 2001) has been used for fast neutrons. Stone (2000) polynomial has been used to  
777 determine surface production rate at the sampling geographic coordinates assuming a SLHL  
778 production rate of  $4.49 \text{ at.g}^{-1}.\text{yr}^{-1}$  for  $^{10}\text{Be}$  with 6% of uncertainty.  $^{10}\text{Be}$  ages have been  
779 calculated using Cosmocalc (Vermeesh 2007). About 10-30 pebbles with centimetre size have  
780 been generally collected for the amalgamated samples of the profiles. Anar samples ages

781 differ slightly from those published in Le Dortz et al. (2009) because they have been  
782 recalculated with updated half-life and attenuation length.

783

784

785 Table A.1: The table presents the measured and calculated parameters used to compare depth-  
786 profile and surface concentrations for different abandonment ages ( $t_{\text{Max}}$  obtained from the  
787 profile rejuvenation method,  $t_{\text{min}}$ , obtained from the youngest surface pebble and  $t_{\text{OSL}}$  when  
788 OSL ages are available) of each analyzed alluvial terrace, T2, T3, and T1. The excess  
789 concentrations correspond to the concentrations remaining in depth-profile samples after  
790 using the rejuvenation method. For each depth-profile sample, adding up this excess  
791 concentration to the concentration corresponding to the *in-situ* surface duration ( $t_{\text{Max}}$ ;  $t_{\text{min}}$  or  
792  $t_{\text{OSL}}$ ) permit to calculate the profile  $^{10}\text{Be}$  concentration converted to the surface for each  
793 abandonment age. This concentration would correspond for each depth-profile sample to their  
794 concentration if they had emplaced and remained at the surface ; it can be compared to the  
795 concentrations measured in the surface samples. Correcting the excess concentration for  
796 radioactive decay allows calculating the  $^{10}\text{Be}$  inheritance in each depth-profile sample, which  
797 corresponds to the inheritance value at the time of the alluvial aggradation.

798

**Highlights**

- Surface and depth profile cosmogenic sampling
- If scattering of concentrations (profile & surface), there is variable inheritance
- If erosion is negligible, we use profile rejuvenation method
- Minimum inheritance, hence, maximum abandonment age for the surface is obtained

Samples	Sample description	Density (g.cm <sup>-3</sup> )	Thickness (cm)	Latitude (°N)	Longitude (°E)	Elevation (m)	Stone scaling factor	Measured <sup>10</sup> Be (10 <sup>5</sup> at.g <sup>-1</sup> SiO <sub>2</sub> )	zero inheritance zero erosion <sup>10</sup> Be model age (ka)
<b>Terrace T2 (Dehshir South)</b>									
<b>Surface sampling</b>									
DS06S32	cobble (10 cm)	2.2	5	30.4476	54.12655	1622	2.78	21.01±0.52	175.57±11.39
DS06S34	cobble (20 cm)	2.2	6	30.44765	54.12751	1619	2.77	21.95±0.32	184.19±11.38
DS06S36	cobble (20 cm)	2.2	6	30.447	54.1284	1620	2.77	15.08±0.24	124.58±7.73
DS08S111	cobble (10 cm)	2.2	6	30.44792	54.13517	1612	2.76	18.52±0.49	154.99±10.15
DS08S112	cobble (10 cm)	2.2	7	30.44793	54.13371	1615	2.76	22.12±0.60	186.22±12.26
DS08S113	cobble (10 cm)	2.2	7	30.44708	54.13213	1618	2.77	26.61±0.68	225.76±14.73
DS08S114	cobble (10 cm)	2.2	6	30.44803	54.13074	1623	2.78	6.16±0.17	49.87±3.29
<b>Profile sampling</b>									
DS08P126	amalgam 30 cm below ground surface	2.2	-	30.44823	54.12648	1645	2.82	11.23±0.30	
DS08P127	amalgam 60 cm below ground surface	2.2	-	30.44823	54.12648		2.82	6.10±0.17	
DS08P128	amalgam 100 cm below ground surface	2.2	-	30.44823	54.12648		2.82	5.82±0.16	
DS08P129	amalgam 150 cm below ground surface	2.2	-	30.44823	54.12648		2.82	5.91±0.16	
DS08P130	amalgam 210 cm below ground surface	2.2	-	30.44823	54.12648		2.82	8.86±0.24	
DS08P131	amalgam 270 cm below ground surface	2.2	-	30.44823	54.12648		2.82	3.62±0.10	
DS08P132	amalgam 370 cm below ground surface	2.2	-	30.44823	54.12648		2.82	4.31±0.12	
<b>Terrace T3 (Dehshir North)</b>									
<b>Surface sampling</b>									
DN06S2	2 fragments of the same gelyfracted cobble	2.2	3	30.64065	54.01907	1550	2.66	26.55±3.66	235.55±35.38
DN06S6	cobble (10 cm)	2.2	5	30.64036	54.021083	1550	2.66	51.88±0.72	489.51±30.15
DN06S7	cobble (15 cm)	2.2	4	30.64045	54.02092	1550	2.66	48.78±1.19	456.66±29.58
DN06S10	cobble (10 cm)	2.2	5	30.6405	54.020917	1550	2.66	49.21±0.69	461.15±28.42
DN06A11	Amalgam (20 pluricentimetric clasts)	2.2	-	30.6405	54.020917	1550	2.66	48.37±0.66	452.25±27.83
DN06S19	cobble (10 cm)	2.2	4	30.64208	54.02502	1550	2.66	46.84±0.65	436.33±26.88
DN06S21	cobble (10 cm)	2.2	4	30.64189	54.02503	1550	2.66	54.60±0.75	518.71±31.93
DN06S23	cobble (10 cm)	2.2	7	30.64177	54.0251	1550	2.66	50.72±2.12	477.09±34.88
DN06S26	cobble (10 cm)	2.2	8	30.64101	54.02506	1550	2.66	46.99±1.02	437.88±27.94
DN06S28	cobble (20 cm)	2.2	9	30.64038	54.02512	1550	2.66	45.92±0.99	426.74±27.23
<b>Profile sampling</b>									
DN06P12Q	amalgam 25 cm below ground surface	2.2	-	30.64114	54.02133	1550	2.66	33.77±0.85	
DN06P13Q	amalgam 55 cm below ground surface	2.2	-	30.64114	54.02133		2.66	25.80±0.66	
DN06P14Q	amalgam 95 cm below ground surface	2.2	-	30.64114	54.02133		2.66	22.12±0.45	
DN06P15Q	amalgam 165 cm below ground surface	2.2	-	30.64114	54.02133		2.66	13.60±0.34	
DN06P16Q	amalgam 230 cm below ground surface	2.2	-	30.64114	54.02133		2.66	6.89±0.17	
DN06P17Q	amalgam 270 cm below ground surface	2.2	-	30.64114	54.02133		2.66	4.37±0.07	
DN06P18Q	amalgam 305 cm below ground surface	2.2	-	30.64114	54.02133		2.66	9.68±0.24	

**Terrace T1 (Anar)****Surface sampling**

AS06S73	Amalgam - pluricentimetric fragment	2.2	-	31.19474	55.15243	1574	2.73	7.86 ± 0.18	64.27 ± 4.12
AS06S74	Amalgam - pluricentimetric fragment	2.2	-	31.19404	55.15357	1562	2.71	3.93 ± 0.12	31.86 ± 2.16
AS06S75	3 fragments of the same gelyfracted pebble	2.2	4	31.19263	55.15304	1571	2.73	2.20 ± 0.05	17.45 ± 1.12
AS06S76	conglomerate with pebbles of quartz (cm)	2.2	9	31.19405	55.15330	1559	2.71	2.55 ± 0.06	20.34 ± 1.30
AS08S89	fragment of a cobble	2.2	5	31.20095	55.15331	1571	2.73	3.53 ± 0.086	28.90 ± 1.87
AS08S91	several fragments of the same gelyfracted pebble	2.2	-	31.19915	55.15242	1571	2.73	3.47 ± 0.08	28.40 ± 1.84
AS08S92	Amalgam - pluricentimetric fragment	2.2	-	31.19874	55.15221	1570	2.73	3.96 ± 0.10	32.50 ± 2.11
AS08S94	two fragments of the same gelyfracted pebble	2.2	6	31.19391	55.15297	1570	2.73	5.20 ± 0.12	42.74 ± 2.77
AS08S95	pebble (10 cm)	2.2	6	31.19499	55.15471	1570	2.73	2.70 ± 0.067	22.06 ± 1.43
AS08S96	pebble (10 cm)	2.2	5	31.19358	55.15577	1570	2.73	3.83 ± 0.10	31.45 ± 2.08

**Profile sampling**

AS08P97	amalgam 370 cm below ground surface	2.2	-	31.19526	55.15340	1567	2.72	4.29 ± 0.12	
AS08P98	amalgam 270 cm below ground surface	2.2	-	31.19527	55.15341		2.72	3.48 ± 0.09	
AS08P99	amalgam 170 cm below ground surface	2.2	-	31.19527	55.15341		2.72	4.21 ± 0.11	
AS08P100	amalgam 100 cm below ground surface	2.2	-	31.19527	55.15341		2.72	2.24 ± 0.06	
AS08P101	amalgam 70 cm below ground surface	2.2	-	31.19527	55.15341		2.72	5.15 ± 0.14	
AS08P102	amalgam 30 cm below ground surface	2.2	-	31.19527	55.15341		2.72	3.8 ± 0.10	
AS08P108	amalgam 150 cm below ground surface	2.2	-	31.19527	55.15341		2.72	1.8 ± 0.05	

**T2****T2 Surface**

Samples	Depth (cm)	Measured $^{10}\text{Be}$ ( $10^5 \text{ at.g}^{-1}\text{SiO}_2$ )
DS06S32	0	21.01±0.52
DS06S34	0	21.95±0.32
DS06S36	0	15.08±0.24
DS08S111	0	18.52±0.49
DS08S112	0	22.12±0.60
DS08S113	0	26.61±0.68
DS08S114	0	6.16±0.17

**T2 Depth profile**

Abandonment age	Samples	Depth (cm)	Abandonment age	Excess concentration ( $10^5 \text{ at.g}^{-1}\text{SiO}_2$ )	$^{10}\text{Be}$ inheritance ( $10^5 \text{ at.g}^{-1}\text{SiO}_2$ )	Profile $^{10}\text{Be}$ concentration converted to surface ( $10^5 \text{ at.g}^{-1}\text{SiO}_2$ )
107 ka	DS08P126	30	107 ka	2.15±0.06	2.27±0.06	15.74±0.42
	DS08P127	60		0	0	13.59±0.37
	DS08P128	100		2.18±0.06	2.30±0.06	15.77±0.44
	DS08P129	150		3.96±0.11	4.17±0.12	17.54±0.48
	DS08P130	210		7.86±0.21	8.29±0.22	21.45±0.57
	DS08P131	270		3.05±0.08	3.22±0.09	16.64±0.47
	DS08P132	370		4.31±0.12	4.00±0.11	4.22±0.12
50 ka	DS08P126	30	50 ka	6.92±0.19	7.10±0.19	13.09±0.35
	DS08P127	60		3.21±0.09	3.29±0.09	9.37±0.25
	DS08P128	100		4.09±0.11	4.19±0.12	10.25±0.30
	DS08P129	150		8.38±0.13	5.11±0.14	11.15±0.31
	DS08P130	210		3.35±0.26	8.59±0.23	14.54±0.39
	DS08P131	270		4.16±0.09	3.44±0.09	9.51±0.27
	DS08P132	370		4.31±0.12	4.16±0.12	4.27±0.12
30 ka	DS08P126	30	30 ka	8.63±0.23	8.76±0.23	12.44±0.33
	DS08P127	60		4.36±0.12	4.42±0.12	8.17±0.22
	DS08P128	100		4.78±0.13	4.85±0.14	8.59±0.24
	DS08P129	150		5.35±0.14	5.43±0.15	9.16±0.25
	DS08P130	210		8.57±0.23	8.70±0.23	12.38±0.31
	DS08P131	270		3.46±0.09	3.51±0.10	7.27±0.21
	DS08P132	370		4.31±0.12	4.21±0.12	4.28±0.12

**T3****T3 Surface**

Samples	Depth (cm)	Measured $^{10}\text{Be}$ ( $10^5 \text{ at.g}^{-1}\text{SiO}_2$ )
DN06S2	0	26.55±3.66
DN06S6	0	51.88±0.72
DN06S7	0	48.78±1.19
DN06S10	0	49.21±0.69
DN06A11	0	48.37±0.66
DN06S19	0	46.84±0.65
DN06S21	0	54.60±0.75
DN06S23	0	50.72±2.12
DN06S26	0	46.99±1.02
DN06S28	0	45.92±0.99

**T3 Depth profile**

Samples	Depth (cm)	Measured $^{10}\text{Be}$ ( $10^5 \text{ at.g}^{-1}\text{SiO}_2$ )	Abandonment age	Excess concentration ( $10^5 \text{ at.g}^{-1}\text{SiO}_2$ )	$^{10}\text{Be}$ inheritance ( $10^5 \text{ at.g}^{-1}\text{SiO}_2$ )	Profile $^{10}\text{Be}$ concentration converted to surface ( $10^5 \text{ at.g}^{-1}\text{SiO}_2$ )
DN06P12Q	25	33.77±0.85	412 ka	0	0	45.53±1.15
DN06P13Q	55	25.80±0.66		3.84±0.09	4.71±0.12	49.36±1.25

DN06P14Q	95	22.12±0.45		9.04±0.18	11.10±0.22	54.56±1.10
DN06P15Q	165	13.60±0.34		8.04±0.20	9.88±0.24	53.57±1.33
DN06P16Q	230	6.89±0.17		4.12±0.10	5.06±0.13	49.65±1.25
DN06P17Q	270	4.37±0.07		2.43±0.04	2.99±0.05	47.96±0.77
DN06P18Q	305	9.68±0.24		8.18±0.20	10.06±0.25	53.71±1.33
DN06P12Q	25	33.77±0.85	235 ka	13.68±0.34	15.38±0.39	40.28±1.01
DN06P13Q	55	25.80±0.66		12.73±0.33	14.32±0.36	39.33±1.00
DN06P14Q	95	22.12±0.45		14.33±0.29	16.12±0.33	40.93±0.83
DN06P15Q	165	13.60±0.34		10.29±0.25	11.57±0.29	36.89±0.91
DN06P16Q	230	6.89±0.17		5.24±0.13	5.89±0.15	31.84±0.80
DN06P17Q	270	4.37±0.07		3.22±0.05	3.62±0.06	29.82±0.48
DN06P18Q	305	9.68±0.24		8.79±0.22	9.89±0.24	35.39±0.87

**T1****T1 Surface**

Samples	Depth (cm)	Measured <sup>10</sup> Be (10 <sup>5</sup> at.g <sup>-1</sup> SiO <sub>2</sub> )
AS06S73	0	7.86 ± 0.18
AS06S74	0	3.93 ± 0.12
AS06S75	0	2.20 ± 0.05
AS06S76	0	2.55 ± 0.06
AS08S89	0	3.53 ± 0.086
AS08S91	0	3.47 ± 0.08
AS08S92	0	3.96 ± 0.10
AS08S94	0	5.20 ± 0.12
AS08S95	0	2.70 ± 0.067
AS08S96	0	3.83 ± 0.10

**T1 Depth profile**

Samples	Depth (cm)	Measured <sup>10</sup> Be (10 <sup>5</sup> at.g <sup>-1</sup> SiO <sub>2</sub> )	Abandonment age	Excess concentration (10 <sup>5</sup> at.g <sup>-1</sup> SiO <sub>2</sub> )	<sup>10</sup> Be inheritance (10 <sup>5</sup> at.g <sup>-1</sup> SiO <sub>2</sub> )	Profile <sup>10</sup> Be concentration converted to surface (10 <sup>5</sup> at.g <sup>-1</sup> SiO <sub>2</sub> )
AS08P97	370	4.29 ± 0.12	46 ka	4.16±0.11	4.26±0.12	9.80±0.27
AS08P98	270	3.48 ± 0.09		3.24±0.09	3.32±0.09	8.88±0.24
AS08P99	170	4.21 ± 0.11		3.55±0.09	3.64±0.10	9.19±0.25
AS08P100	100	2.24 ± 0.06		0.70±0.02	0.72±0.02	6.34±0.17
AS08P101	70	5.15 ± 0.14		2.89±0.08	2.96±0.08	8.53±0.23
AS08P102	30	3.8 ± 0.10		0	0	5.64±0.15
AS08P108	150	1.8 ± 0.05		0.97±0.03	0.99±0.03	6.61±0.19
AS08P97	370	4.29 ± 0.12	17.5 ka	4.24±0.12	4.28±0.12	6.44±0.17
AS08P98	270	3.48 ± 0.09		3.39±0.09	3.42±0.09	5.59±0.15
AS08P99	170	4.21 ± 0.11		3.95±0.11	3.99±0.11	6.15±0.17
AS08P100	100	2.24 ± 0.06		1.63±0.04	1.65±0.05	3.83±0.11
AS08P101	70	5.15 ± 0.14		4.26±0.12	4.30±0.12	6.46±0.17
AS08P102	30	3.8 ± 0.10		2.29±0.06	2.31±0.06	4.49±0.12
AS08P108	150	1.8 ± 0.05		1.47±0.04	1.48±0.04	3.67±0.10
AS08P97	370	4.29 ± 0.12	10 ka	4.26±0.12	4.29±0.12	5.49±0.15
AS08P98	270	3.48 ± 0.09		3.43±0.09	3.45±0.09	4.66±0.13
AS08P99	170	4.21 ± 0.11		5.07±0.11	4.09±0.11	5.30±0.14
AS08P100	100	2.24 ± 0.06		1.90±0.05	1.91±0.05	3.13±0.08
AS08P101	70	5.15 ± 0.14		4.65±0.13	4.68±0.12	5.88±0.16
AS08P102	30	3.8 ± 0.10		2.96±0.08	2.97±0.08	4.18±0.11
AS08P108	150	1.8 ± 0.05		1.61±0.05	1.62±0.05	2.28±0.08

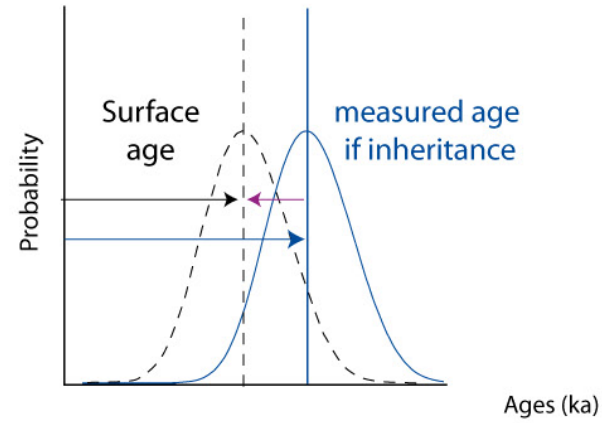
Figure 1

a)

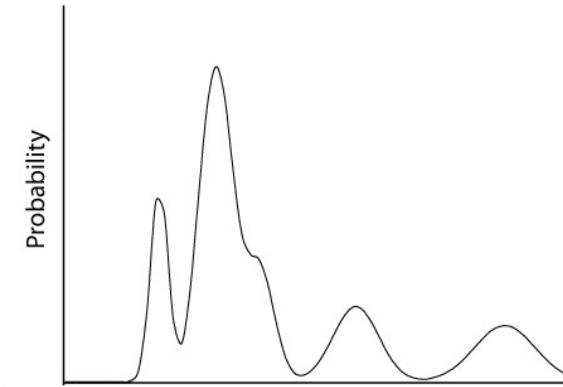
surface sampling only



b)

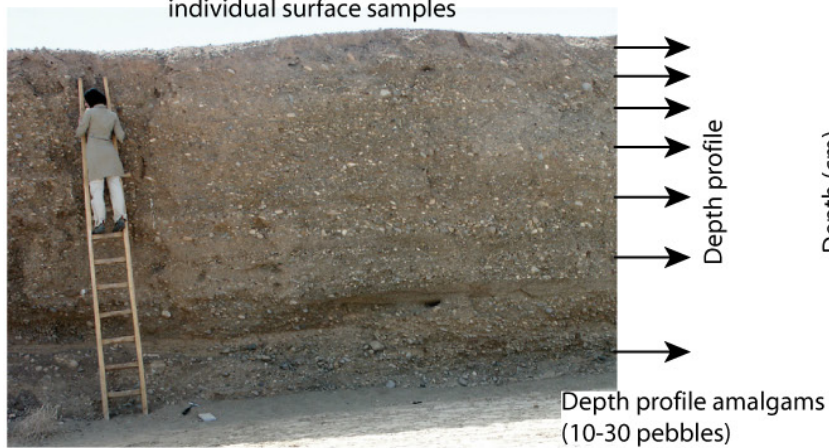


c)



surface and depth profile sampling

individual surface samples



inheritance

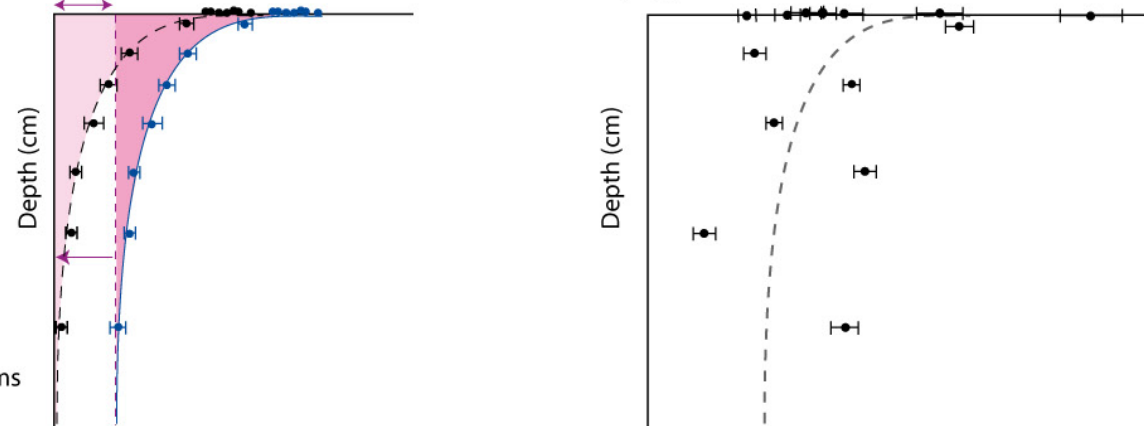
Concentration  $^{10}\text{Be}$  (at/g)

Figure 2

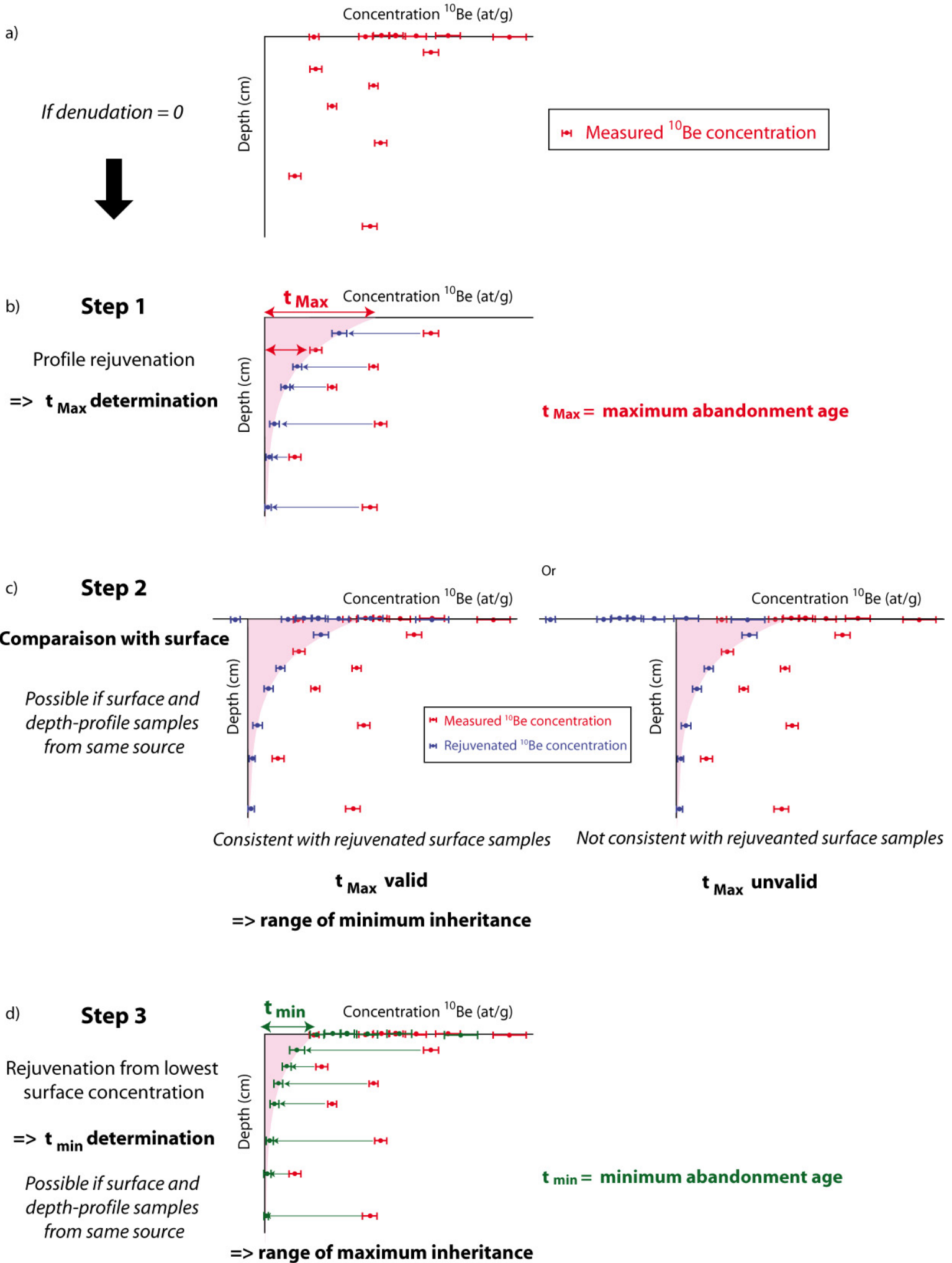


Figure 3

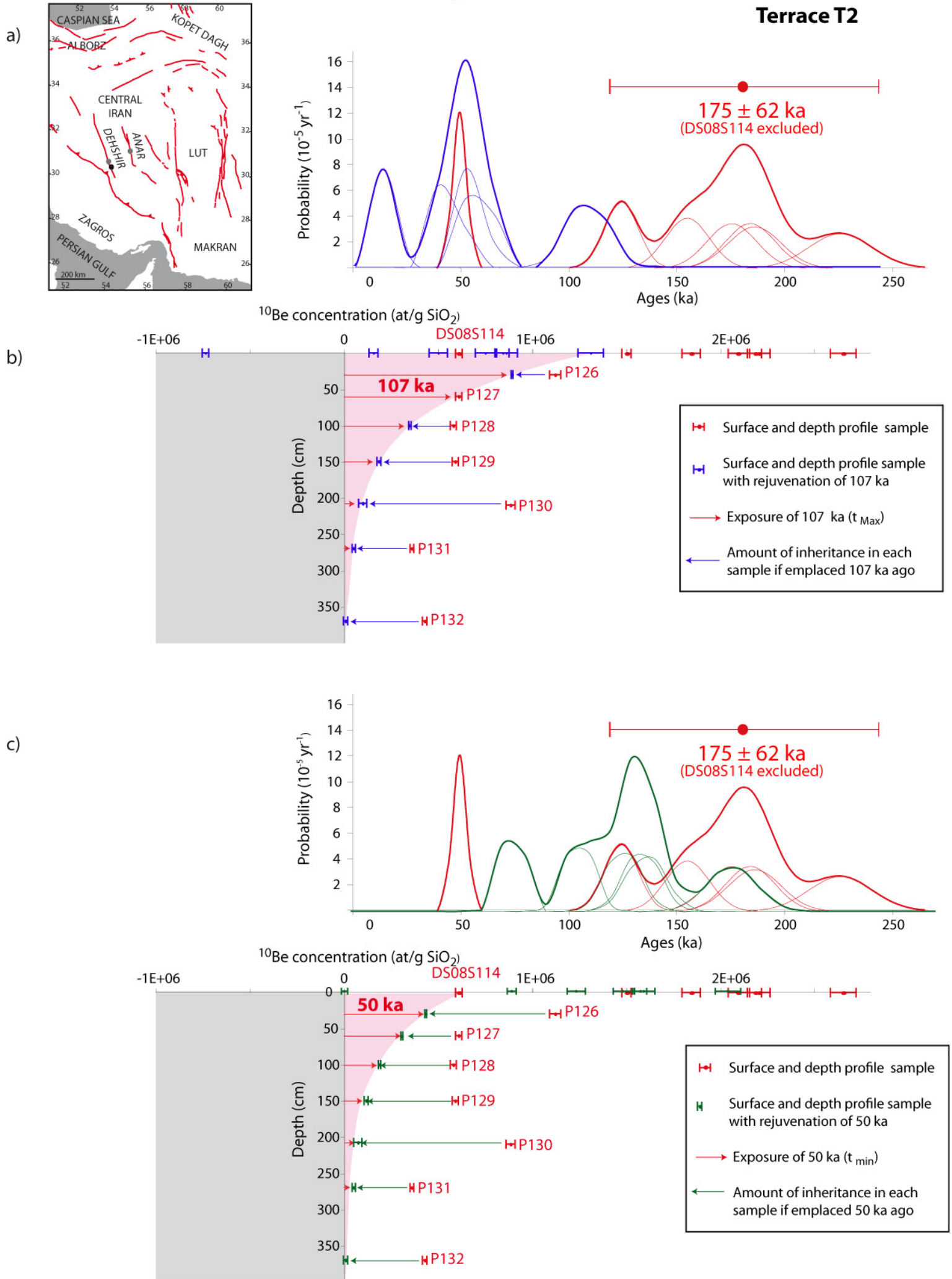


Figure 4

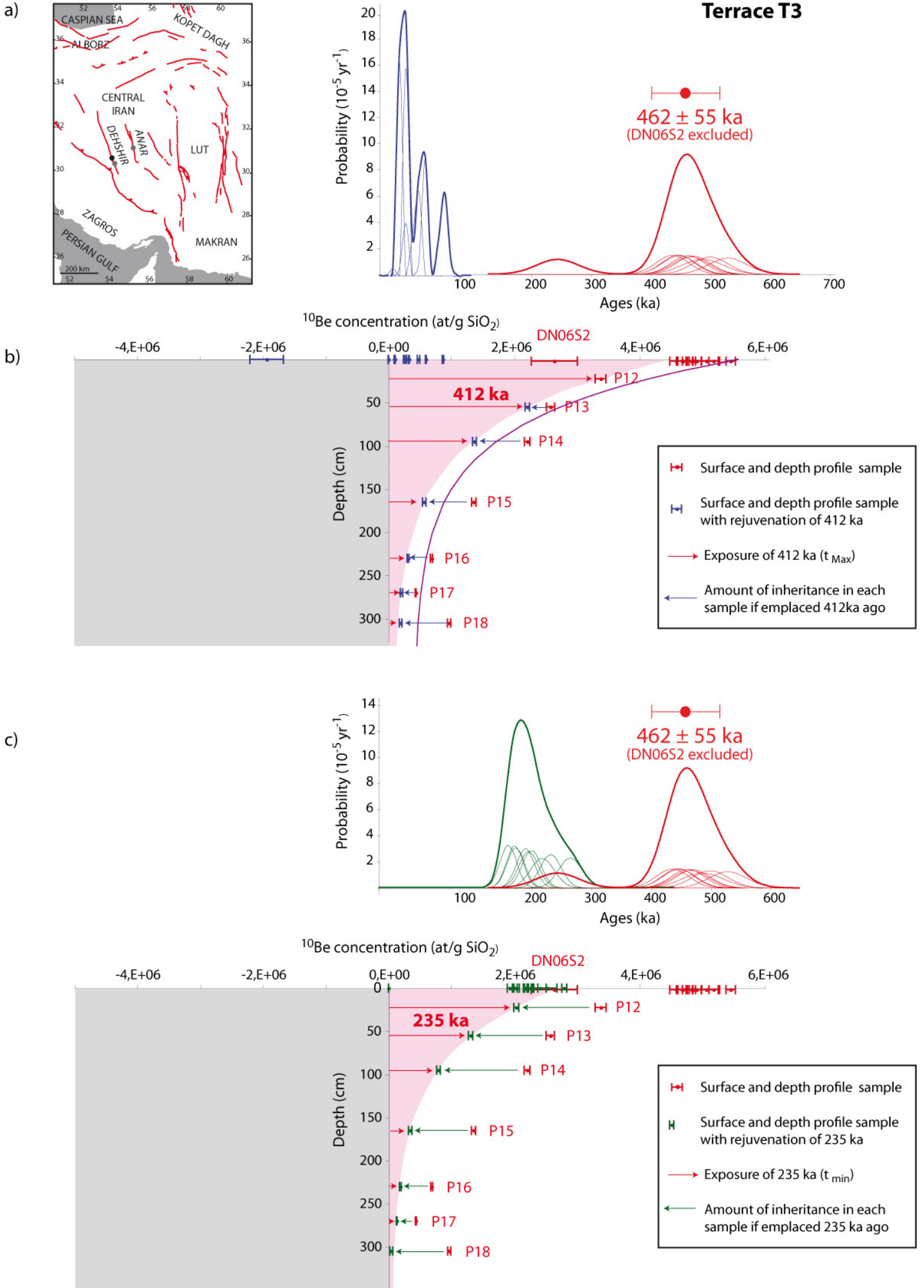


Figure 5

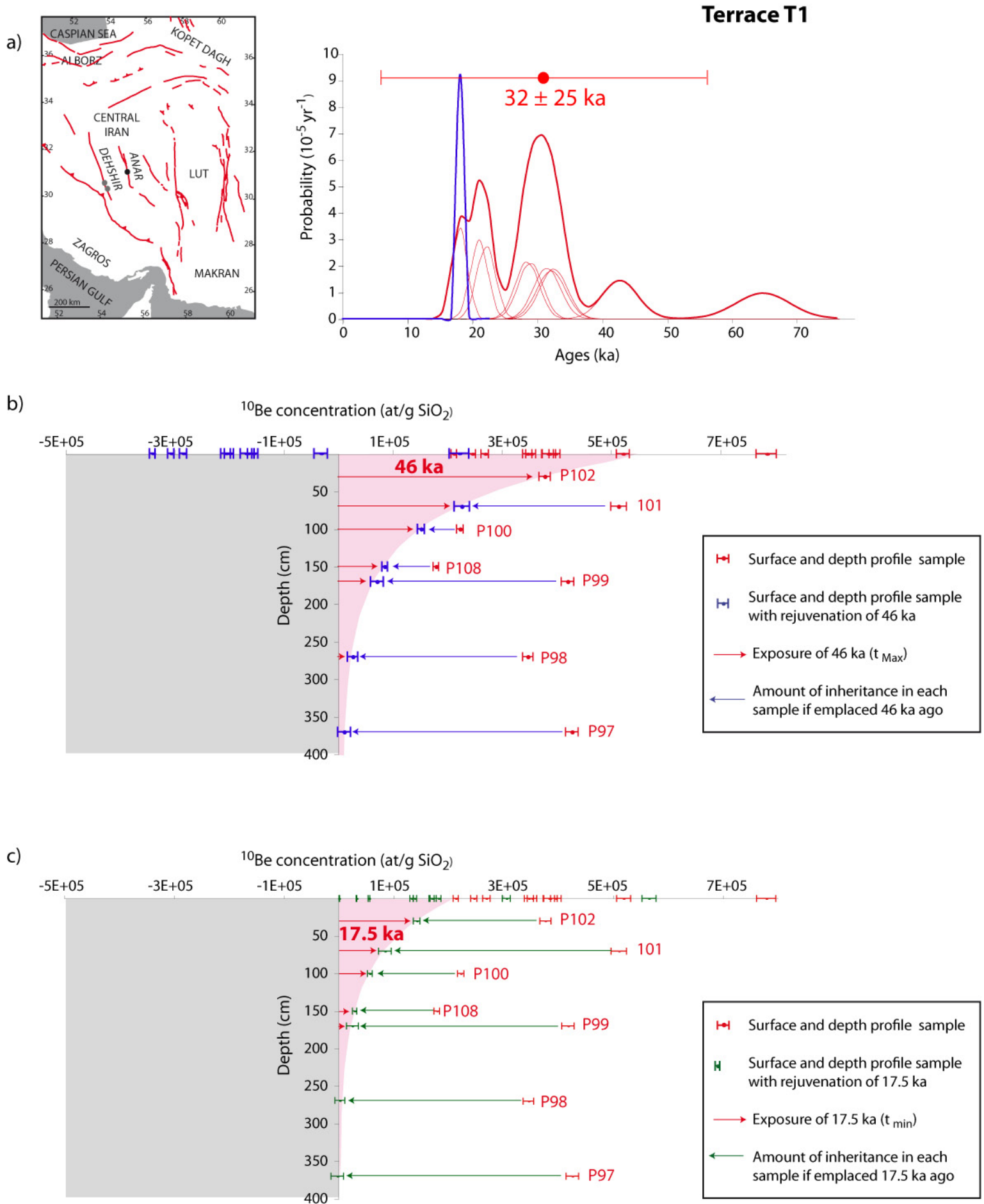


Figure A1

Terrace T2

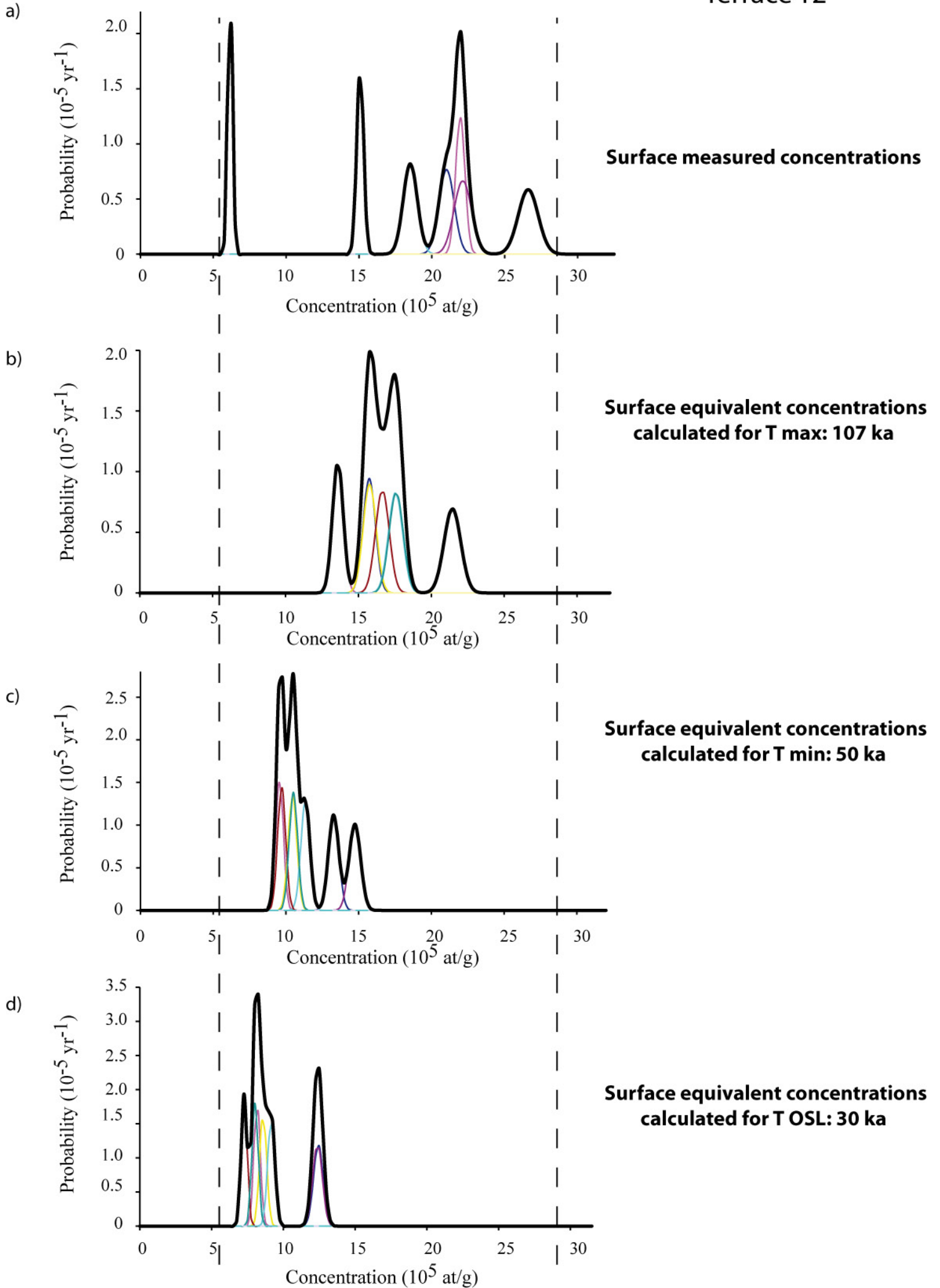


Figure A2

Terrace T3

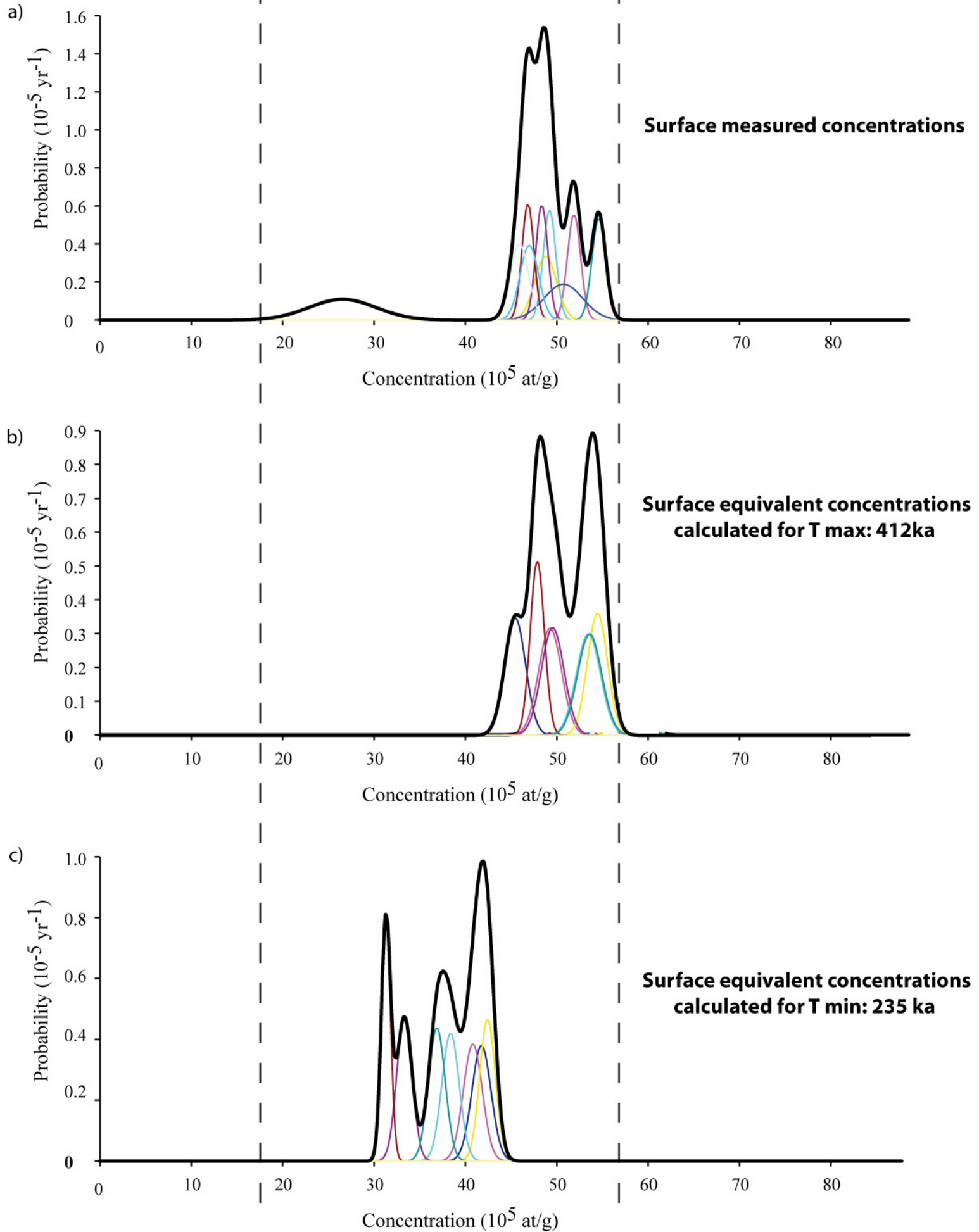


Figure A3

Terrace T1 (Anar)

